Mathematisches Forschungsinstitut Oberwolfach

Report No. 59/2013

DOI: 10.4171/OWR/2013/59

Material Theories

Organised by
Antonio DeSimone, Trieste
Stephan Luckhaus, Leipzig
Lev Truskinovsky, Palaiseau

15 December – 21 December 2013

Abstract. The subject of this meeting was mathematical modeling of strongly interacting multi-particle systems that can be interpreted as advanced materials. The main emphasis was placed on contributions attempting to bridge the gap between discrete and continuum approaches, focusing on the multi-scale nature of physical phenomena and bringing new and nontrivial mathematics. The mathematical debates concentrated on nonlinear PDE, stochastic dynamical systems, optimal transportation, calculus of variations and large deviations theory.

Mathematics Subject Classification (2010): 74Axx, 74Bxx, 74Cxx, 74Nxx, 74Qxx, 74Rxx, 76Rxx, 76Sxx, 76Txx, 76S05, 80xx.

Introduction by the Organisers

New mathematics usually originates from problems suggested by the neighboring fields of science. In this sense this interdisciplinary workshop is a unique asset for the mathematical community and it plays an important role of the incubator of new ideas, allowing participants to transform physical insight into rigorous mathematical theories.

The goal of the meeting was to expose the mathematics community to new and exciting developments in the fields of Mechanics of Materials, Statistical Physics and Biology. The subjects discussed at the workshop were quite diverse, ranging from martensitic phase transitions and ductile fracture to plant morphogenesis, unicellular swimmers, and active matter.

The program included 21 keynote lectures, and considerable time was given to discussions initiated by the talks. Among the topics raising particular interest

were: new methods of analysis of the buckling of cylindrical shells by Y. Grabovsky, new approaches to ductile fracture by M. Ortiz, new perspectives on Hadamard compatibility condition by J. Ball, microscopic theory of pre-stress in binary alloys by P. Smereka, insights into the origin of configurational forces through experiments on elastic structures by D. Bigoni, study of microstructures based on optimal scaling of the energy by F. Otto and F. Theil and a discrete theory of surface energy in crystals by P. Rosakis. An interesting discussion of dislocation mechanics was initiated by two talks: by A. Garroni, from the point of view of modern calculus of variations and by A. Yavari from the point of view of geometric mechanics. G. Francfort presented a new perspective on homogenization in macroscopic plasticity. T. Lelievre reviewed recent progress in the theory of accelerated methods in molecular dynamics. A novel method of capturing both coarse grained behavior and fluctuations by using the theory of large deviations and Gamma convergence was presented by M. Peletier. A. Mielke showed the possibility of re-writing reaction-diffusion systems as flows with a gradient structure, provided that detailed balance is satisfied. Y. Brenier discussed a new class of minimization problems under rearrangement constraints, originally motivated by a problem in fluid mechanics related to stationary solutions of 2D Euler equations. The asymptotic behavior of thin bodies was the subject of two talks: by G. Bouchitte in the nonlinear elasticity framework and by B. Audoly in plasticity theory. B. Schmidt reported new results in the problem of simultaneous geometric linearization and homogenization of multi-well energy functionals. Finally, biology was represented by theories of plant growth (A. Boudaoud) , cell motility (M. Arroyo) and collective interactions in bacterial suspensions (E. Clement).

By exposing participants to a broad spectrum of subjects and techniques, all centered on the mechanics and thermodynamics of materials, the workshop created an atmosphere conducive to new collaboration between researchers with complementary expertise who had little chances to cross paths otherwise. The organizers were able to witness the success of this idea from the liveliness of the discussions during and after the talks, and from the active involvement and enthusiastic response of junior participants. This workshop has been in the past a source of many collaborations and this one promises to be no exception.

Workshop: Material Theories

Table of Contents

Mark A. Peletier (joint with Upanshu Sharma and Manh Hong Duong)
Coarse-graining and fluctuations: Two birds with one stone 3437

Eric Clément (joint with Gaston Mino, Jeremie Gachelin, Annie Rousselet, Anke Lindner)
Hydrodynamics of active bacterial fluids 3440

Felix Otto
Optimal Martensitic Inclusions 3443

Davide Bigoni (joint with Federico Bosi, Francesco Dal Corso, and Diego Misseroni)
Eshelby-like forces in elastic structures 3443

Tony Lelièvre
Mathematical analysis of accelerated dynamics 3444

Yann Brenier
Minimization under rearrangement constraints: a gradient flow approach 3447

Peter Smereka (joint with Arvind Baskaran, Christian Ratsch)
Inability of Continuum Theory to Evaluate the Elastic Energy of Alloys 3449

Arezki Boudaoud (joint with co-authors in papers cited)
Stochasticity in plant growth and morphogeneseis 3452

Marino Arroyo (joint with Antonio DeSimone)
The euglenoid movement in nature and for shape control of active surfaces 3454

Alexander Mielke (joint with Matthias Liero, Giuseppe Savaré)
Gradient structures and dissipation distances for reaction-diffusion systems 3455

John Ball (joint with Carsten Carstensen)
Hadamard's compatibility condition for microstructures 3458

Yury Grabovsky (joint with Davit Harutyunyan)
Buckling of axially compressed circular cylindrical shells 3460

Florian Theil (joint with David Bourne, Mark Peletier)
Energy-driven pattern formation via competing long- and short-range interactions 3463

Michael Ortiz (joint with Sergio Conti, Landry Fokoua)
Optimal Scaling in Ductile Fracture 3463

Bernd Schmidt (joint with Martin Jesenko)
Closure and commutability results for Gamma-limits and an application to multi-well energy functionals 3465

Gilles A. Francfort (joint with Alessandro Giacomini)
Periodic Homogenization in Elasto-Plasticity 3468

Arash Yavari (joint with Alain Goriely)
Non-Riemannian geometries and the nonlinear mechanics of distributed defects 3470

Basile Audoly (joint with John W. Hutchinson)
The effect of the unloading response on the necking of elastic bars 3472

Guy Bouchitté (joint with J.J Alibert, I.Fragalà, I.Lucardesi)
Do optimal thin rods contain homogenized regions? 3473

Adriana Garroni (joint with Roberto Alicandro, Lucia De Luca, Marcello Ponsiglione)
Metastability and dynamics of discrete topological singularities via Gamma-convergence: Application to dislocations 3476

Phoebus Rosakis
Lattice Point Problems and the Surface Energy of Crystals 3480

Abstracts

Coarse-graining and fluctuations: Two birds with one stone

Mark A. Peletier
(joint work with Upanshu Sharma and Manh Hong Duong)

It is well known how a duality relation of the type

$$I^\varepsilon(\rho) = \sup_f J^\varepsilon(\rho, f)$$

can yield the inequality $\liminf_{\varepsilon\to 0} I^\varepsilon(\rho^\varepsilon) \geq I^0(\rho^0)$ when ρ^ε converges to ρ^0 in a topology for which $J^\varepsilon(\cdot, f)$ is continuously convergent. This idea is the basis for many Gamma-convergence results. In this talk I described how this idea can be combined with the concepts of *coarse-graining* and *large deviations* to give a natural context in which to formulate and prove the convergence statements that constitute rigorous coarse-graining.

We illustrate the method on a simple abstract case. Given a sequence of i.i.d. $\mathcal{X}$-valued stochastic Markov processes $X^{\varepsilon,i}$, indexed by $i = 1, 2, \dots$ and $\varepsilon > 0$, we define the *empirical measure* $\rho^{n,\varepsilon}$ as the t-parametrized curve of measures

$$\rho^{n,\varepsilon} : [0,T] \to \mathcal{P}(\mathcal{X}), \qquad \rho_t^{n,\varepsilon} = \frac{1}{n}\sum_{i=1}^n \delta_{X_t^{\varepsilon,i}}. \tag{1}$$

For many systems of this type it has been proven that $\rho^{n,\varepsilon}$ satisfies the *large-deviation principle*

$$\mathrm{Prob}\big(\rho^{n,\varepsilon}\big|_{[0,T]} \approx \rho^\varepsilon\big|_{[0,T]}\big) \sim \exp\big[-nI^\varepsilon(\rho^\varepsilon)\big] \qquad \text{as } n\to\infty, \text{ for fixed } \varepsilon, \tag{2}$$

with a characterization of the rate function I^ε in the form (1); see e.g. [3].

The rate functional I^ε characterizes not only the probability of fluctuations, through (2), but also the probability-1 behaviour: this corresponds to the equation $I^\varepsilon(\rho) = 0$, which has exactly one solution, given by the equation $\partial_t \rho_t = (A^\varepsilon)^T \rho_t$. Here A^ε is the generator of the processes $X^{\varepsilon,i}$.

While we describe the situation here for i.i.d. processes, many generalizations are available for interacting particle systems; the ideas of this talk apply to many of these systems as well.

We define *coarse-graining* as the shift to a reduced description through a *coarse-graining map* $\Pi : \mathcal{X} \to \mathcal{Y}$, which typically is highly non-injective; the challenge is to characterize the behaviour of the stochastic processes $Y^{\varepsilon,i} := \Pi(X^{\varepsilon,i})$ in the limit $\varepsilon \to 0$. Note that the coarse-grained equivalent of $\rho : [0,T] \to \mathcal{P}(\mathcal{X})$ is the push-forward $\hat\rho := \Pi_\# \rho : [0,T] \to \mathcal{P}(\mathcal{Y})$.

The central idea of this talk is contained in the following calculation:

$$\begin{array}{lcl} I^\varepsilon(\rho^\varepsilon) & = & \sup_f \; J^\varepsilon(\rho^\varepsilon, f) \\ & \overset{f=g\circ\Pi}{\geq} & \sup_g \; J^\varepsilon(\rho^\varepsilon, g\circ\Pi) \\ & \overset{(*)}{=:} & \sup_g \; \widehat{J}^\varepsilon(\hat{\rho}^\varepsilon, g) \\ & & \qquad\qquad \Big\downarrow \varepsilon \to 0 \\ \widehat{I}^0(\hat{\rho}^0) & \overset{(**)}{:=} & \sup_g \; \widehat{J}^0(\hat{\rho}^0, g) \end{array}$$

The inequality above arises from the reduction to a subset of all functions f, namely those that are of the form $f = g \circ \Pi$. The critical step is $(*)$: here one requires that the combination of loss-of-information in passing from ρ^ε to $\hat{\rho}^\varepsilon$ is consistent with the loss-of-resolution in considering only functions $f = g \circ \Pi$. This step essentially requires a proof of *local equilibrium*; it states that the behaviour of ρ^ε is such that the missing information can be deduced from the push-forward $\hat{\rho}^\varepsilon$, at least approximately in the limit $\varepsilon \to 0$. This is at the heart of many coarse-graining methods, it is often laborious, and usually it can not be avoided.

Assuming that $\widehat{J}^\varepsilon(\cdot, g)$ converges in an appropriate manner to some $\widehat{J}^0(\cdot, g)$, we then define $\widehat{I}^0$ by duality in terms of $\widehat{J}^0$ as in $(**)$. Whether or not $\widehat{I}^0$ is the rate functional of some stochastic process can not be answered at this level of abstraction, and is to be determined case by case.

We now make the discussion more concrete by considering a specific system. Consider the stochastically perturbed Hamiltonian system

$$dQ = \frac{1}{\varepsilon} P \, dt, \tag{3a}$$

$$dP = -\frac{1}{\varepsilon} \nabla V(Q) \, dt + \sqrt{2} \, dW, \tag{3b}$$

where P, Q take values in $\mathbb{R}$, $V \in C^2(\mathbb{R})$ is a given potential with quadratic growth, and W is a standard Wiener process. The stochastic differential equation (3) describes a single conservative degree of freedom, such as a particle in a well or an anharmonic oscillator, with non-conservative noise; the noise appears only in the second equation, which is a force balance.

For the purposes of illustration we will choose the double-well potential $V(q) = (q^2 - 1)^2/4$. With this choice the Hamiltonian $H(q, p) = p^2/2 + V(q)$ also has a double-well-structure, as is shown in Figure 1.

Without the noise, the system is deterministic and preserves the Hamiltonian $H(q, p) = p^2/2 + V(q)$, and solutions follow level sets of H. With noise, however, the Hamiltonian is not preserved, and the solutions follow a stochastic path that stays more or less close to a level curve, depending on the size of ε.

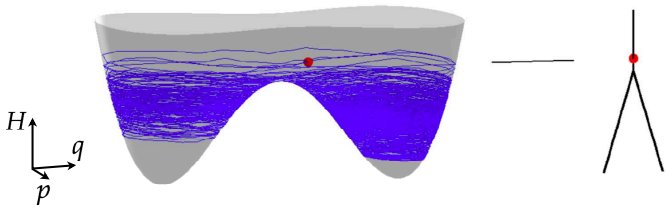

FIGURE 1. A single run of the SDE (3). The graph on the right-hand side is a reduction of the state space $\mathbb{R}^2$, according to the map Π; see the text for details.

We will be interested in the limit $\varepsilon \to 0$; in this limit there is a separation of time scales, in which the solutions have a fast H-conserving drift, and follow level sets very closely over $O(\varepsilon)$ times, with velocity $O(1/\varepsilon)$; at $O(1)$ time scales the value of H changes, and performs a biased Brownian motion, as was first proved by Freidlin and Wentzell [4]. We re-prove this result as an illustration of the method.

We write $X^\varepsilon = (Q^\varepsilon, P^\varepsilon)$ for the process in $\mathbb{R}^2$ described by the SDE (3) with a deterministic initial datum $x_0 \in \mathbb{R}^2$, and we consider a sequence $X^{\varepsilon,i}$, $i = 1, 2, \ldots$ of i.i.d. copies of this process. For this system Cattiaux and Léonard [1] prove the large-deviation principle (2) and the characterization (1).

The coarse-graining map Π maps $\mathbb{R}^2$ to the *graph* Γ consisting of equivalence classes of level sets of H, under the equivalence relation of belonging to the same connected component of the level sets of H. Below the saddle-point each level set has two connected components, thus leading to the two prongs in the graph Γ. For this system the method described above yields:

Theorem 1.
- $\hat{\rho}^\varepsilon \longrightarrow \hat{\rho}^0$ *as* $\varepsilon \to 0$ *in* $C([0,T]; \mathcal{P}(\Gamma))$*;*
- $\liminf_{\varepsilon\to 0} I^\varepsilon(\rho^\varepsilon) \geq \widehat{I}^0(\hat{\rho}^0)$.

The liminf inequality in this theorem implies a type of convergence of solutions: the projected stochastic processes $Y^\varepsilon = \Pi(X^\varepsilon)$ converge to biased diffusions on the graph Γ, and their behvaviour is fully characterized by the law $\mu \in \mathcal{P}(\Gamma)$ that uniquely satisfies $\widehat{I}^0(\mu) = 0$. This equation can be shown to be equivalent to the diffusion-process description of [4], and to a weak-solution concept for a PDE.

REFERENCES

[1] P. Cattiaux and C. Léonard. Minimization of the Kullback information of diffusion processes. *Ann. Inst. H. Poincaré Probab. Statist.*, 30(1):83–132, 1994.
[2] M. H. Duong, M. A. Peletier, and U. Sharma. In preparation.
[3] J. Feng and T. G. Kurtz. *Large deviations for stochastic processes*, volume 131 of *Mathematical Surveys and Monographs*. American Mathematical Society, 2006.
[4] M. I. Freidlin and A. D. Wentzell. *Random Perturbations of Hamiltonian Systems*. American Mathematical Society, 1994.

Hydrodynamics of active bacterial fluids

Eric Clément
(joint work with Gaston Mino, Jeremie Gachelin, Annie Rousselet, Anke Lindner)

From the hydrodynamics point of view, assemblies of microscopic swimmers dispersed in a fluid at very low Reynolds number, display emergent properties differing strongly from those of passive suspensions [1]. Balances of momentum and energy as well the constitutive transport properties, are deeply modified by the momentum sources distributed in the bulk. The swimming autonomy of those organisms implies that, no external force or torque will be exerted on the fluid at large distances. Therefore, the leading hydrodynamics should be governed - at most- by a force-dipole representing the long range swimmer influence. As a consequence, depending on the dipole polarity, many micro-organisms can be cast into two categories: swimmer pushers or "swimmer pullers" [2]. For example, bacteria propelled by flagella at their rear, as Escherichia-coli or bacillus-subtilis, are pushers. On the other hand, unicellular algae such as Chlamydomonas reinhardtii, propelling via a couple of deforming frontal flagella, are pullers. Finally, in recent years, progresses have been made on the synthesis of active colloids using Janus-like reactive properties at their surface, to move autonomously [3]. For the last system, the classification in terms of long range hydrodynamics is not clearly established. The presence of living and apparently gregarious entities offers the possibility to move collectively in order to organize and synchronize, at a mesoscopic level [4]. These collective effects can have two origins; either from short range interactions and dipolar orientation such as in flocks and herds models [5] or, via long range hydrodynamic coupling as in semi-diluted particulate fluids [6]. A primary consequence of this organization will be to yield anomalous statistical behavior either in the spatial distribution of swimmers or in their velocity correlations. These mesoscopic organization properties will have a strong influence on the macroscopic constitutive relations and can be at the origin of complex dynamical patterns. The situation of long range hydrodynamic coupling is certainly the least studied theoretically, essentially due to the difficulty to solve the full N-body hydrodynamic interactions; a question that remains timely also in the case of passive suspensions. However in recent years have emerged new results, based on simplified numerical simulations of active swimmers in association with diluted or semi diluted theories for active suspensions . Numerically and theoretically, there have been several propositions in order to simplify the bacteria representation by a force dipole and a short range repulsive structure modeled for example, as pushed ellipsoids, slender bodies or active spheres. A central question is the complexity of the trajectories undertaken by the bacteria themselves. These trajectories can be governed either by an internal logic, often based on a local probing of the environmental chemistry and decisions on the motion direction (chemotaxis), or by mechanical transduction based on long-or short range interactions mediated by the fluid. For the moment, we ignore if the effect of mechanical interactions is just

passive or if there is any transduction between mechanical and biological signals that would lead to a retroaction on the way the microorganisms swim.

- **Enhanced Brownian motion of a passive tracer in a bacterial bath**: to tackle the open and timely question of the physical nature of a bacterial bath, we compared the behavior of two kinds of active micrometric swimmers: E-Coli bacteria and artificial self-propelling rods, moving close to a solid surface [7]. This study follows the pioneering work of Wu and Libchaber [8] who provided evidences of an activated Brownian motion for bacteria suspensions trapped in a thin film. In our group, for both the E-Coli and the artificial swimmer, the motion was followed as well as its ability to activate, beyond Brownian motion, passive tracers, hence characterizing the active momentum transfer to the fluid. The resulting diffusion coefficient was found for bacteria and artificial swimmers, to be the sum of a thermal Brownian contribution near the wall and an active part : $D = D_B + \beta V_B n$, where D_B is the Brownian diffusivity , β a coefficient scaling as the bacteria size at the power 4 and n the number of active bacteria swimming aroud the surface. Importantly, to reach this result, a quantitative discrimination have to be made between "active" and "diffusive" swimmer trajectories. In a more recent contribution [9]we have shown that this result can be simply understood in an hydrodynamic framework, as the compound of elementary encounters between the active swimmers and the tracers. The β a coefficient being directly related to the "swimming efficiency", the less efficent is the swimmer the higher is its contribution to the active diffusivity.

- **Active rheology of bacteria suspensions** : active suspensions can collectively acquire original constitutive properties. For example for pushers, at low shear rate, the viscosity can even be smaller than the suspending fluid viscosity. This is due to the dipolar contribution enhancing shear when the bacterium is oriented at$\pi/4$with respect to the shearing direction [10, 11, 12]. Thus, the relation between effective viscosity and shear rate would depends crucially on the angular distribution of the force-dipole director. One experiment on viscous relaxation of a bacillus subtillis suspensions trapped in a film probed a significant viscosity reduction [13]. However there were no direct measurement of the full rheology relations. This is the reason why we recently designed a system to measure the viscosity of a wild type E-Coli suspension in the dilute and semi-dilute limits using a microfluidic device build as a Y shape micro-fluidic channel [14]. We used a Y-shape microfluidic device to compare the viscosities of two liquids at low shear. On one arm, the active suspension is injected and on the other arm, the suspending fluid in injected at the same flow rate. From the position of the interface between the pure fluid and the suspension, one may extract the suspension relative viscosity. We obtained an effective viscosity which shows a non-Newtonian response. Varying the bacteria density and the flow rate, we display a regime specific to active fluids, where the relative viscosity is lower than the viscosity of the suspending viscous fluid. We also managed using a fast camera coupled to the microscope , to obtain the vertical profiles for the bacteria density and the corresponding velocity

distributions for both the fluid and the bacteria by monitoring the trajectories of the bacteria and some passive tracers.

- **Onset of collective motion** : using the direct visualization possibilities of microfluidic channels, we investigated the emergence of collective motion in the bulk of an active suspension of E. coli bacteria. When increasing the concentration from a dilute to a semi-dilute regime, we observe a continuous cross-over from a dynamical cluster regime to a regime of 'bio-turbulent' convection patterns [15]. We measure a length scale characterizing the collective motion as a function of the bacteria concentration. For bacteria fullly supplied with oxygen, the increase of the correlation length is almost linear with concentration and at the largest concentrations tested, the correlation length could be as large as 24 bacterial body sizes (or 7-8 when including the flagella bundle). In contrast, under conditions of oxygen shortage the correlation length saturates at a much smaller size .

References

[1] A.Baskaran andC. Marchetti, *Statistical mechanics and hydrodynamics of bacterial suspensions*, PNAS **106** (2009), 15567.

[2] Lauga E. and T. R. Powers, *The hydrodynamics of swimming microorganisms*, Rep. Prog. Phys.**32** (1990), 096601.

[3] Y. Wang et al., *Bipolar Electrochemical Mechanism for the Propulsion of Catalytic Nanomotors in Hydrogen Peroxide Solution*, Langmuir **22** (2006), 10451.

[4] Koch D.L. and G Subramanian, *Collective hydrodynamics of swimming micro-organisms: Living fluids*, Ann. Rev. Fluid Mech. **43** (2011), 637.

[5] T. Vicsek, A. Zafeiris, *Collective motion*, Physics Reports**517** (2012), 71.

[6] D. Saintillan, M. Shelley *Active suspensions and their nonlinear models*, C. R. Physique **14** (2013), 497.

[7] G. Mino, T. E. Mallouk, T. Darnige, M. Hoyos, J. Dauchet, J. Dunstan, R. Soto, Y. Wang, A. Rousselet, and E. Clement, *Enhanced Diffusion due to Active Swimmers at a Solid Surface*, Phys. Rev. Lett. **106** (2011), 048102.

[8] Wu X-L and A.Libchaber, *Particle Diffusion in a Quasi-Two-Dimensional Bacterial Bath*, Phys. Rev. Lett. **84** (2000), 3017 .

[9] G.Mino, J. Dunstan, A. Rousselet, E. Clement, R.Soto, *Induced Diffusion of Tracers in a Bacterial Suspension: Theory and Experiments*, J. Fluid Mech **729** (2013), 423.

[10] Hatwalne Y, Ramaswamy S, Rao M, Aditi Simha R , *Rheology of active-particle suspensions*,Phys Rev Lett **92** (2004) 118101.

[11] Haines M., A. Sokolov, I. S. Aranson, L. Berlyand, and D. A. Karpeev, *Three-dimensional model for the effective viscosity of bacterial suspensions*,Phys Rev E **80** (2009) 041922 .

[12] Saintillan D., *The dilute rheology of swimming suspensions: A simple kinetic model*, Model Exp. Mech. **50** (2010) 1275 .

[13] Sokolov A. and Aranson I., *Reduction of Viscosity in Suspension of Swimming Bacteria*, Phys. Rev. Lett . **103** (2009) 148101 .

[14] J.Gachelin, G.Mino, H. Berthet A.Lindner, A.Rouselet, E.Clement, *Non-Newtonian active viscosity of E-coli suspensions*, Phys. Rev. Lett. **110** (2013), 268103.

[15] J.Gachelin, A.Rousselet, A.Lindner, E.Clement, *Collective motion in E. coli bacteria suspensions*, New Journal of Physics, in press (2014).

Optimal Martensitic Inclusions

Felix Otto

This is joint work with Hans Knüpfer and Robert V. Kohn. We consider the cubic-to-tetragonal phase transition in shape memory alloys in the geometrically linear description with interfacial energy. We are interested in the scaling of the minimal energy as a function of the volume V of the martensite inclusion. We see this as a contribution to understanding the critical volume of microstructured martensite nuclei at a given temperature or loading. We have two results:

(1) If we allow for all 3 Martensitic variants the energy scales as $V^{9/11}$.
(2) If one of the two variants is supressed, the energy scales $V^{11/13}$.

The difference in the exponents highlight the effect of self-accommodation which is only possible if all three variants are allowed (in equal volume fraction).

Eshelby-like forces in elastic structures

Davide Bigoni
(joint work with Federico Bosi, Francesco Dal Corso, and Diego Misseroni)

The Eshelbian force is the main concept of a celebrated theoretical frame- work associated with the motion of dislocations, phase transforming boundaries, and defects in solids. In a similar vein, in an elastic structure where a (smooth and bilateral) constraint can move and release energy, a force driving the configuration change is generated, which therefore is called by anal- ogy Eshelby-like or configurational. This force (generated by a specific movable constraint) can be derived via variational calculus or through an asymptotic approach. Its action on the elastic structure is counterintuitive, but is fully substantiated and experimentally measured on a model structure that has been designed, realized and tested.

In another model structure, an elastic rod subject to a dead compressive load at the free end penetrates into a sliding sleeve, ending with a linear elastic spring. Bifurcation and stability analysis of this simple elastic system shows a variety of unexpected behaviours: (i.) an increase of buckling load at decreasing of elastic stiffness; (ii.) a finite number of buckling loads for a system with infinite degrees of freedom (leading to a non-standard Sturm-Liouville problem); (iii.) more than one bifurcation loads associated to each bifurcation mode; (iv.) a restabilization of the straight configuration after the second bifurcation load associated to the first instability mode; (v.) the presence of an Eshelby-like (or configurational) force, deeply influencing stability.

The reported findings open a new perspective in the mechanics of deformable mechanisms, with possible broad applications, even at the nanoscale.

References

[1] D. Bigoni, F. Dal Corso, F. Bosi and D. Misseroni. Eshelby-like forces acting on elastic structures: theoretical and experimental proof. *Mech. Materials*, doi: http://dx.doi.org/10.1016/j.mechmat.2013.10.009, 2013.

[2] D. Bigoni, F. Dal Corso, F. Bosi and D. Misseroni. Instability of a penetrating blade. *J. Mech. Phys. Solids*, in press, 2014.

Mathematical analysis of accelerated dynamics

Tony Lelièvre

The aim of molecular dynamics simulations is to understand the relationships between the macroscopic properties of a molecular system and its atomistic features. In particular, one would like to evaluate numerically macroscopic quantities from models at the microscopic scale. Applications are numerous, ranging from biology to chemistry and materials science.

Models for molecular dynamics are built at the atomistic level. The positions of N particles (atoms) are stored in a vector $X_t \in \mathbb{R}^{3N}$ and this vector evolves using a potential function $V : \mathbb{R}^{3N} \to \mathbb{R}$ which models the interaction between the particles. Stochastic terms are added to model the fact that the system is at a given temperature T. A prototypical dynamics (which is a simplification of the phase-space Langevin dynamics which is used in practice) is the overdamped Langevin:

$$dX_t = -\nabla V(X_t)\, dt + \sqrt{2\beta^{-1}} dW_t \tag{1}$$

where $\beta^{-1} = k_B T$ (k_B being the Boltzmann constant) and W_t is a $3N$-dimensional Brownian motion. The dynamics (1) is used to compute either thermodynamic quantities (averages with respect to the canonical measure $\mu(dx) = Z^{-1} \exp(-\beta V(x))\, dx$, approximated by trajectorial averages using ergodicity) or dynamical quantities (averages over trajectories). In both cases, one reason which makes these computations difficult is metastability.

Metastability refers to the fact that the solution to (1) remains trapped for very long times in some regions of the configurational space. These trapping regions are called metastable states. This is related to a timescale problem: the typical timescale at the microscopic level, to discretize the dynamics (1), is the femtosecond ($10^{-15}\, s$) whereas the macroscopic timescales of interest, which correspond to jumping events from one metastable state to another are of the order of microseconds to seconds. Metastability may come from energetic barriers (X_t has to go through a saddle point to leave a metastable region which is in the vicinity of a local minimum of V) or entropic barriers (X_t has to find its way through a narrow corridor to leave a large flat region). Because of metastability, trajectorial averages have to be considered over very long times to get good approximations of thermodynamic quantities, and transitions between metastable states are very difficult to simulate (these are rare events).

A natural idea in this context is to try to replace the original dynamics by a state-to-state dynamics which will only reproduce the jumps between the metastable states. Hopefully, this coarse-grained dynamics will be Markovian, so that one would obtain an excellent description of the original dynamics using a simple discrete state space Markovian dynamics (called a kinetic Monte Carlo model or a

Markov state model in this context). The basic question is then: in which situation the exit event from a metastable state satisfies the basic two requirements of a Markovian transition:

- the exit time is exponentially distributed
- and is independent of the next visited state.

The answer is the following: if the stochastic process X_t remains for a sufficiently long time in a region $W \subset \mathbb{R}^{3N}$ (assumed to be bounded in the following), then these two properties are satisfied. This can be formalized using the notion of quasi-stationary distribution (see the third property below).

The quasi-stationary distribution ν associated to the dynamics (1) and attached to a domain W is defined by:

$$\forall t > 0, \forall A \subset W, \nu(A) = \frac{\int_W \mathbb{P}(X_t^x \in A,\, t < T_W^x)\, \nu(dx)}{\int_W \mathbb{P}(t < T_W^x)\, \nu(dx)} \tag{2}$$

where X_t^x denotes the solution to (1) starting from x. In words, if $X_0 \sim \nu$ and if $(X_s)_{0 \leq s \leq t}$ has not left the region W, then $X_t \sim \nu$. Let us give three important properties of the quasi-stationary distribution. The first property is that, under appropriate assumptions, if X_t starts in W, then

$$\lim_{t \to \infty} \mathcal{L}(X_t | T_W > t) = \nu \tag{3}$$

where $T_W = \inf\{t \geq 0,\, X_t \notin W\}$ and $\mathcal{L}(X_t | T_W > t)$ thus denotes the law of X_t conditionally to the fact that the process remains in W in the time interval $[0, t]$. A second property is that $\nu(dx) = u_1(x)\, dx$ where u_1 is the first eigenfunction of $L^* = \mathrm{div}(\nabla V + \beta^{-1}\nabla)$ with absorbing boundary conditions:

$$\begin{cases} L^* u_1 = -\lambda_1 u_1 \text{ on } W, \\ \quad u_1 = 0 \text{ on } \partial W. \end{cases} \tag{4}$$

A third property is that if $X_0 \sim \nu$, then

- the first exit time T_W from W is exponentially distributed with parameter λ_1 ;
- T_W is independent of the first hitting point X_{T_W} on ∂W ;
- the exit point distribution is proportional to $-\partial_n u_1$: for all smooth test functions $\varphi : \partial W \to \mathbb{R}$,

$$\mathbb{E}^\nu(\varphi(X_{T_W})) = -\frac{\int_{\partial W} \varphi\, \partial_n u_1\, d\sigma}{\beta\lambda \int_W u_1(x)\, dx}. \tag{5}$$

From a theoretical viewpoint, the interest of this point of view is that one can better understand and quantify metastabiliy. For example a metastable region can be defined as a region such that the typical time to reach the limit (3) is much smaller than the typical time to exit W. One can also use the tools from semi-classical analysis to understand the exit events in the small temperature regime, and in particular to justify the transition state theory which is used by chemists to study exit events using the height of surrounding barriers. This can be an alternative to more standard approaches based on large deviation techniques,

potential theoretic approaches, or semi-classical analysis for the operator on the whole configurational space.

From a numerical viewpoint, A. Voter built in the late nineties algorithms to very efficiently generate state-to-state dynamics starting from Langevin dynamics [5, 6, 4]. These algorithms consist in using the fact that the stochastic process remains trapped for a very long time in a metastable state, in order to generate very efficiently the exit event from this state. Three ideas have been used.

First, using the fact that starting from ν, T_W is exponentially distributed and independent from X_{T_W}, the *parallel replica* method [6] consists in simulating many independent trajectories starting from ν in parallel and to consider the first exit event from W among the replicas. A statistically correct exit event is then obtained, by simply multiplying the first exit time by the number of replicas. This strategy is very versatile, and does not require any specific assumption on the process (except the fact that it indeed remains trapped for a very long time in W before using this procedure). In particular, it is adapted to both energetic and entropic barriers. We refer to [2] for more details.

The two other methods require a small temperature assumption, and only apply to energetic barriers. In the *hyperdynamics* [5], the idea is to raise the local minimum of the potential V in W in order to accelerate the exit event. The question is then how the pair $\left(\lambda_1, \frac{\partial_n u_1}{\int_{\partial W} \partial_n u_1}\right)$ which fully describes the exit event (see the third property above) depends on the potential V. It can be shown (see [3]) that, under appropriate assumption (in particular the biasing potential δV is zero on ∂W), there exists $c > 0$ such that, in the limit $\beta \to \infty$,

$$\frac{\lambda_1(V+\delta V)}{\lambda_1(V)} = \frac{\int_W e^{-\beta V}}{\int_W e^{-\beta(V+\delta V)}}(1+\mathcal{O}(e^{-\beta c}))\,,$$
$$\frac{\partial_n\left[u_1(V+\delta V)\right]\big|_{\partial W}}{\|\partial_n\left[u_1(V+\delta V)\right]\|_{L^1(\partial W)}} = \frac{\partial_n\left[u_1(V)\right]\big|_{\partial W}}{\|\partial_n\left[u_1(V)\right]\|_{L^1(\partial W)}} + \mathcal{O}(e^{-\beta c}) \quad \text{in } L^1(\partial W),$$

where we explicitly indicate with obvious notation the dependency of the pair $\left(\lambda_1, \frac{\partial_n u_1}{\int_{\partial W} \partial_n u_1}\right)$ on the potential (either the original one V, or the biased potential $V+\delta V$). Using these estimates, one simply has to multiply the exit time observed on the biased potential by the computable boost factor $\frac{\int_W e^{-\beta V}}{\int_W e^{-\beta(V+\delta V)}}$ in order to get a statistically correct exit event.

Finally, in the so-called *temperature accelerated dynamics* [4], the idea is to increase the temperature and to infer what would have happened at low temperature from the exit events observed at high temperature. The justification of the algorithm is still on-going work, even if some progress has been made on simple one-dimensional situations [1].

References

[1] T. Lelièvre D. Aristoff. Mathematical analysis of temperature accelerated dynamics, 2013. http://arxiv.org/abs/1305.6569.

[2] C. Le Bris, T. Lelièvre, M. Luskin, and D. Perez. A mathematical formalization of the parallel replica dynamics. *Monte Carlo Methods Appl.*, 18(2):119–146, 2012.
[3] T. Lelièvre and F. Nier. Low temperature asymptotics for quasi-stationary distributions in a bounded domain, 2013. `http://arxiv.org/abs/1309.3898`.
[4] M.R. Sorensen and A.F. Voter. Temperature-accelerated dynamics for simulation of infrequent events. *J. Chem. Phys.*, 112(21):9599–9606, 2000.
[5] A.F. Voter. A method for accelerating the molecular dynamics simulation of infrequent events. *J. Chem. Phys.*, 106(11):4665–4677, 1997.
[6] A.F. Voter. Parallel replica method for dynamics of infrequent events. *Phys. Rev. B*, 57(22):R13 985, 1998.

Minimization under rearrangement constraints: a gradient flow approach

Yann Brenier

We start with the following minimization problem under rearrangement constraints that comes from mathematical fluid mechanics [3, 4, 2]:
Given a scalar function φ_0 on a smooth bounded domain D in $\mathbf{R}^d$, find another function φ, with level sets of same volume as those of φ_0, that minimizes some functional $E[\varphi]$. The problem can be rephrased as a saddle-point problem

$$\inf_{\varphi: D\to\mathbf{R}} \sup_{f:\mathbf{R}\to\mathbf{R}} \quad E[\varphi] + \int_D [f(\varphi(x) - f(\varphi_0(x)]dx. \tag{1}$$

Our main example for E is the Dirichlet integral

$$E[\varphi] = \frac{1}{2}\int_D |\nabla\varphi(x)|^2 dx. \tag{2}$$

In this case, optimal solutions of (1) are formally solutions to $-\triangle\varphi + f'(\varphi) = 0$ for some function $f : \mathbf{R} \to \mathbf{R}$, and, in 2D, are just stationary solutions to the Euler equations of incompressible fluids. This problem has also an interesting discrete counterpart. After discretizing the Dirichlet integral on a lattice with N grid points A_i, we have to find a permutation σ that achieves

$$\inf_{\sigma} \sum_{i,j=1,N} c_{\sigma_i\sigma_j}\lambda_{ij}\ , \quad c_{ij} = |\varphi_0(A_i) - \varphi_0(A_j)|^2$$

for a suitable matrix λ that depends on the lattice. This belongs to the class of "quadratic assignment problems", a well known class of NP combinatorial optimization problems which includes the famous traveling salesman problem.

To address problem (1), we suggest a "gradient flow" approach involving a time dependent function $\varphi_t(x)$ starting from $\varphi_0(x)$ at $t = 0$. Hopefully, as $t \to +\infty$, φ_t will reach a solution to our minimization problem. A canonical way to preserve the volume of each level set is the transport of φ by a time-dependent divergence-free velocity field $v = v_t(x) \in \mathbf{R}^d$, parallel to ∂D, according to

$$\partial_t\varphi_t + \nabla\cdot(v_t\varphi_t) = 0, \ \ \nabla\cdot v_t = 0, \quad v_t//\partial D \tag{3}$$

(which just means, when v is smooth, $\varphi_t(\xi_t(x)) = \varphi_0(x)$, where ξ is the time-dependent family of volume and orientation-preserving diffeomorphisms of D generated by v through: $\partial_t \xi_t(x) = v_t(\xi_t(x)),\ \xi_0(x) = x$).
We denote by Sol(D) the Hilbert space of all divergence free L^2 vector fields on D and parallel to ∂D and introduce a lsc convex functional K on Sol(D). We denote by K^* its Legendre-Fenchel transform $K^*(g) = \sup_w((g,w)) - K(w)$. For all pairs (φ, v) subject to (3), we formally get

$$\frac{d}{dt}E[\varphi_t] = -((G_t, v_t)), \quad G_t = \mathbf{P}(E'[\varphi_t]\nabla\varphi_t), \tag{4}$$

where we denote by $((\cdot,\cdot))$ the L^2 inner product, by E' the gradient of E with respect to the L^2 metric and by $\mathbf{P}$ the L^2 projection onto Sol(D). Thus,

$$\frac{d}{dt}E[\varphi_t] + K[v_t] + K^*[G_t] = \eta[G_t, v_t], \quad \eta[g,w] = K[w] + K^*[g] - ((g,w)),$$

where the right-hand side η is always nonnegative and vanishes if and only if

$$v_t = K^{*\prime}[G_t], \tag{5}$$

which is the closure equation we suggest to define our "gradient flow" equation, following the ideas of [5] (somewhat in the spirit of [1]). As just seen, this closure equation is equivalent to the differential inequality

$$\frac{d}{dt}E[\varphi_t] + K[v_t] + K^*[G_t] \le 0,$$

or, using the definition of K^* as the Legendre-Fenchel transform of K,

$$\frac{d}{dt}E[\varphi_t] + K[v_t] + ((G_t, z_t)) - K[z_t] \le 0,\ \forall\ z_t \in \text{Sol(D)}. \tag{6}$$

So, our gradient flow is now defined by combining the transport equation (3), definition (4), and either the closure equation (5) or the variational inequality (6), which are formally equivalent.
From now on, let us limit the discussion to the periodic cube $D = \mathbf{T}^d$ and concentrate on the case when E is the Dirichlet integral (2). Then, (4) and (6) respectively read

$$G_t = -\mathbf{P}\nabla\cdot(\nabla\varphi_t \otimes \nabla\varphi_t), \tag{7}$$

$$\frac{d}{dt}||\nabla\varphi_t||^2 + 2K[v_t] + ((\nabla\varphi_t\otimes\nabla\varphi_t, \nabla z_t + \nabla z_t^T)) \le 2K[z_t], \tag{8}$$

for all smooth $z_t \in$ Sol(D). This suggests a "robust" concept of "dissipative solution" for the gradient flow (3,5) (somewhat in the spirit of Lions' dissipative solutions to the Euler equations [6]), by keeping (3) while just integrating (8) on $[0,t]$, for all $t \ge 0$, with a suitable exponential weight, namely:

$$||\nabla\varphi_t||^2 e^{-tr} + \int_0^t \{2K[v_s] + ((\nabla\varphi_s\otimes\nabla\varphi_s, rI_d - \nabla z_s - \nabla z_s^T)) - 2K[z_s]\}e^{-sr}ds \le ||\nabla\varphi_0||^2, \quad \text{for all smooth } z_t \in \text{Sol(D)}. \tag{9}$$

Here $r \geq 0$ is a constant, depending on z, chosen so that

$$(10) \qquad \forall (t,x), \;\; rI_d \geq \nabla z_t(x) + \nabla z_t(x)^T, \;\; \text{in the sense of symmetric matrices,}$$

in order to be sure that inequality (9) only involves convex functionals of (φ, v).

So, following [5], at least in the case: $D = \mathbf{T}^d$,

$$E[\varphi] = \frac{1}{2}\int_{\mathbf{T}^d} |\nabla\varphi(x)|^2 dx, \quad K[v] = \frac{1}{2}\int_{\mathbf{T}^d} |(\nabla)^m v(x)|^2 dx \quad (m = 0, 1, 2, \cdots),$$

it is fairly easy to establish, for the "dissipative" formulation (3,9,10) of (3,5) and for each initial condition φ_0 with finite Dirichlet integral, the existence of a global solution (φ, v) s.t. $(\nabla\varphi, (\nabla)^m v) \in C^0_w(\mathbf{R}_+, L^2(D)) \times L^2(\mathbf{R}_+, L^2(D))$, and its uniqueness whenever (φ, v) is smooth.
Observe that, for $m \geq 1$, the L^2 norm of ∇v_t is square integrable in time. This implies, by DiPerna-Lions ODE theory (see [6]), that each level set of φ_t keeps its volume unchanged during the evolution by (3) (but, unless $m > 1 + d/2$, not necessarily its topology, which is of some interest in view of the minimization problem (1) we started with). However, unless $m > 1 + d/2$, it is unclear to us that (3,5) even admits local smooth solutions.

References

[1] L. Ambrosio, N. Gigli, G. Savaré, *Calculus and heat flow in metric measure spaces and applications to spaces with Ricci bounds from below,* Inventiones 2013, http://cvgmt.sns.it/paper/1645/. .

[2] V.I. Arnold, B. Khesin, *Topological methods in hydrodynamics, Applied Mathematical Sciences, 125,* Springer-Verlag 1998.

[3] T. B. Benjamin, *The alliance of practical and analytical insight into the nonlinear problems of fluid mechanics,* Lecture notes in mathematics 503, 8-29. Springer-Verlag, 1976.

[4] G. R. Burton, *Rearrangements of functions, maximization of convex functionals and vortex rings,* Math. Ann., 276, 225-253, 1987

[5] Y. Brenier, *Topology-preserving diffusion of divergence-free vector fields and magnetic relaxation,* arXiv:1304.4562, to appear in CMP

[6] P.-L. Lions, *Mathematical topics in fluid mechanics. Vol. 1. Incompressible models,* Oxford Lecture Series in Mathematics and its Applications, 3. 1996.

Inability of Continuum Theory to Evaluate the Elastic Energy of Alloys

Peter Smereka

(joint work with Arvind Baskaran, Christian Ratsch)

Here we show that a widely used model of continuum elasticity fails to properly describe the elastic energy of a binary alloy because it fails to include the microscopic strain arising from atomistic scale variations in composition. This

continuum model has it origins in the seminal paper by Cahn [1, 2] where it was shown that for isotropic elasticity the elastic energy can be written as

$$W_c = \frac{\eta^2 E}{1-\nu}\int_V (\theta-\theta_0)^2 dV. \tag{1}$$

In Eq. (1), η is the effective misfit, E is Young's modulus, ν is the Poisson ratio, θ is the composition field of the alloy and θ_0 is its average. This expression shows that for a uniform composition the elastic energy is zero.

However, using a Keating model it has been argued (e.g. Tsao [3]) that for alloys there is microscopic strain even when the composition appears to be macroscopically uniform. The strain energy associated with this microscopic strain can be considered the elastic contribution to the enthalpy of mixing, H. Then one could posit that the elastic energy of the alloy can be written as

$$W = W_c + H. \tag{2}$$

The atomistic scales are captured by H whereas W_c is used for the continuum scales. Thus, in a finely mixed alloy the dominant contribution will come from H and will lessen in favor of W_c as the alloy coarsens. However, in many models H is not explicitly used and if included, it is assumed to be a function of the average concentration. In this work we show that not only is H important, it cannot be considered a function of the average concentration.

We will exactly solve a ball and spring model of a binary alloy system with lattice mismatch (say Si/Ge for ease of exposition) on a simple periodic square lattice in two dimensions with lattice spacing a. Each site on the lattice is occupied by a Si ($\theta_{\ell,j}=0$) or Ge atom ($\theta_{\ell,j}=1$). The Si-Si, Ge-Ge, and Si-Ge bond lengths are denoted as $a_{\rm Si}$, $a_{\rm Ge}$, and $a_{\rm SiGe}=\frac{1}{2}(a_{\rm Si}+a_{\rm Ge})$. The nearest and next-nearest neighbor atoms are connected by Hookean springs with spring constants K_L and K_D. The model we choose is simple enough to be tractable but with the ability to incorporate the discrete nature of the alloy and to account for the microscopic arrangement of its atoms. To simplify the discussion we shall consider the case $K_L = 2K_D$ where the continuum limit gives rises to isotropic elasticity.

When the alloy is in mechanical equilibrium one can show that

$$W = \overline{W} + \widetilde{W}$$

where $\overline{W} = N^2 4K_D(a_{\rm Si} - a + \theta_0(a_{\rm Ge}-a_{\rm Si}))^2$ represents the contribution to the elastic energy if the material was of a uniform composition. $\widetilde{W}$ results from the compositional variations and a lengthy calculation reveals that

$$\widetilde{W} = \frac{K_D(a_{\rm Si}\mu)^2}{N^2}\sum_{\substack{n=0\\(m,n)\neq(0,0)}}^{N-1}\sum_{m=0}^{N-1} G(\alpha m,\alpha n)|\hat{\theta}_{m,n}|^2, \tag{3}$$

where $\alpha = 2\pi/N$, $\hat{\theta}_{m,n}$ is the discrete Fourier transform of $\theta_{\ell,j}$ and G is plotted on Fig. 1. The dependence of $\widetilde{W}$ on θ can be gleaned from Fig. 1. Different regions of the k-space represent different composition profiles. For example, an alloy that is finely intermixed on an atomic scale has weights, $|\hat{\theta}|^2$, concentrated near (π,π),

while for an alloy with variations on continuum length scales the weights are concentrated near $(0, 0)$. It therefore follows from Fig. 1 that finely mixed alloys have more elastic energy than those that are segregated. Although these cases can be viewed as different regions of k-space, typical composition profiles would of course have weights in all regions and no separation of scales. Thus, Fig. 1. also points to the difficulty relying on formulas like Eq. 2, since it is clear that the elastic energy depends on the details of the atomistic arrangement over the full range of length scales.

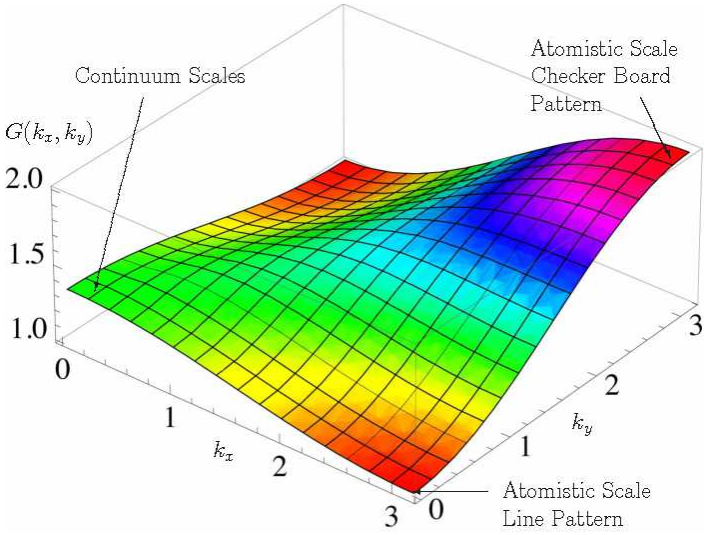

FIGURE 1. A plot of $G(k_x, k_y)$ for the case $K_L = 2K_D$ $(K_D = 1)$

To explore the broader applicability of the ideas discussed above, we perform DFT calculations for Ge/Si (with a zinc-blende lattice). For this we consider various configurations of a $Si_{0.5}Ge_{0.5}$ alloy. We compare bulk alloy composition profiles that resemble a 3-dimensional checkerboard, where each "checker-unit" consists of 1, 8, or 64 atoms of the same type (i.e., all Si or all Ge) occupying a cubic region in space. We do this by placing the configuration in a zinc blend lattice with reference lattice constant a_{Si} or a_{SiGe} and then optimizing the structure. Table 1 summarizes the DFT results. E^{tot} is the total energy (that includes bond and elastic energies) for systems with checker units that consist of N_C atoms, and ΔE^{tot} is the energy difference with respect to a checkerboard with $N_C = 1$. For a system with the lattice constant a_{Si} (which is most relevant for Ge deposition on Si) we find that the checkerboard with $N_C = 8$ is preferred by 1 meV per atom (over a system with $N_C = 1$), and that one with $N_C = 64$ is preferred by 4 meV per atom. For the lattice constant a_{SiGe}, the coarser system with $N_C = 64$ is also preferred, but only by 1 meV. The numbers for $\Delta E^{el}(N_C) = E^{el}(N_C) - E^{el}(N_C =$

1) represent the change in energy per atom after correcting for the fact that simple bond counting arguments favor intermixing and should be considered the true elastic contribution due to coarsening.

TABLE 1. ΔE^{tot} and ΔE^{el} for different values of N_C. Energy changes (in meV) are with respect to a system with $N_C = 1$ (a perfect zinc-blende structure).

N_C	$\Delta E^{\text{tot}}(a_{\text{Si}})$	$\Delta E^{\text{tot}}(a_{\text{SiGe}})$	$\Delta E^{\text{el}}(a_{\text{Si}})$	$\Delta E^{\text{el}}(a_{\text{SiGe}})$
1	0	0		
8	-1	1	-6	-4
64	-4	-1	-11	-8

In summary, we have demonstrated that a widely used continuum theory of elasticity is not able to correctly capture the behavior of the elastic energy of a strained alloy. Our results indicate that finely mixed alloys have more elastic energy than those more coarsely mixed. This is due to the presence of microscopic strain. The more finely mixed the alloy becomes, the more difficult it is to elastically relax. Therefore, intermixing will actually increase the strain energy of alloys and not lower it as predicted by some continuum theories.

REFERENCES

[1] J.W. Cahn, Acta Metallurgica **9**, 795-801 (1961).
[2] P. Fratzl, O. Penrose, and J.L. Lebowitz, J. Stat. Phys. **95**, 1429-1503 (1999).
[3] J.Y. Tsao, Fundamentals of Molecular Beam Epitaxy,Academic Press, New York, 1993. (see Chapter 4).

Stochasticity in plant growth and morphogeneseis

AREZKI BOUDAOUD
(joint work with co-authors in papers cited)

Why are plant leaves generally flat? In our earlier work [1], we investigated the equilibrium configurations of a thin elastic plate endowed with a non-Euclidian metric that decays spatially away from the plate edge. The corresponding PDE has a variational formulation and depends on a small parameter (the plate thickness), raising interest from the applied mathematics community. Using numerical simulations, we found that the energy of the plate has a large number of metastable minima, and that, in many cases, the absolute minimum of the energy corresponds to a fractal-like configuration where the plate has a wrinkled edge, mimicking the shape of leaves such as in ornamental cabbage. In the context of leaves, such non-Euclidian metric can be considered as a proxy for growth. Therefore, maintaining a flat leave requires a specific pattern of growth and mechanisms to ensure that growth is properly coordinated spatially.

As cells within a tissue are relatively independent, each cell can have its own intrinsic growth rate, and gradients in growth rate correspond in gradients in the reference configuration of the elastic body, which generates mechanical stress. How do cells react to such mechanical stress? By combining experiments and solutions of the the corresponding elasticity problems [2, 3], we concluded that mechanical stress induces the mechanical reinforcement of cells (through the synthesis of cellulose microfibrils in the direction of the highest principal stress), which results in slowing down growth in that direction.

In order to study the consequences of this mechanism on growth heterogeneity, we formulated the following problem [4, 5], which combines a simplified version of cell elasticity – corresponding to the difference between actual cell shape and a target (reference) shape – and an evolution equation for the target shape – so as to account for growth. The tissue in 2D is defined by the position of all cell vertices $\{\mathbf{r}_\alpha\} \in \left(\mathbb{R}^2\right)^N$, each cell $i \in \{1, 2, ..., L\}$ being defined by its vertices $\alpha \in \mathbb{A}_i$, with the condition that a given vertex belongs to three cells, except on boundaries. Let $\mathbf{r}_i^{(c)} = \sum_{\alpha\in\mathbb{A}_i} \mathbf{r}_\alpha/\#\mathbb{A}_i$ be the centroid of a cell and $u_{\alpha,i} = \mathbf{r}_\alpha - \mathbf{r}_i^{(c)}$ the reduced positions of the vertices. We characterize cell shape by the 2×2 covariance matrix $M_i = \sum_{\alpha\in\mathbb{A}_i} u_{\alpha,i} \otimes u_{\alpha,i}/\#\mathbb{A}_i$ and the target (reference) shape by a 2×2 real matrix $M_i^{(t)}$. The elastic energy is the defined as

$$\mathcal{E} = \sum_{i=1}^{L} ||M_i - M_i^{(t)}||^2$$

where $||\cdot||$ stands for the 2-norm. The elastic energy is minimized with respect to the positions of the vertices $\mathbf{r}_\alpha$. We note that if the target matrix varies over the tissue, then the configuration has a residual stress, which can be defined as $S_i = M_i - M_i^{(t)}$; its deviatoric part is $D_i = S_i - \mathrm{trace}(M_i)\mathbb{I}$. Heterogeneity of intrinsic growth and the slowing of growth in the direction of the highest stress eigenvalue are translated into an evolution equation of the form

$$\frac{\mathrm{d}M_i^{(t)}}{\mathrm{d}t} = \Gamma_i M_i^{(t)} - \delta(M_i^{(t)} D_i + D_i M_i^{(t)})/2$$

$\{\Gamma_i\}$ is a set of random uncorrelated Gaussian variables with standard deviation γ, which stands for a random intrinsic growth; δ is the strength of the feedback of stress on the texture of the tissue.

We simulated this problem numerically, and we found that, as long as δ is large enough, the actual growth $\left(M_i^{(t)}\right)^{-1} \frac{\mathrm{d}M_i^{(t)}}{\mathrm{d}t}$ increases in spatial heterogeneity when δ increases. This means that, surprisingly, this mechanical feedback enhances growth heterogeneity and that it cannot contribute to the maintenance of flatness in leaves.

References

[1] B. Audoly and A. Boudaoud, *Self-Similar Structures near Boundaries in Strained Systems*, Physical Review Letters **91** (2003), 086105.

[2] O. Hamant, M. Heisler, H. Jonsson, P. Krupinski, M. Uyttewaal, P. Bokov, F. Corson, P. Sahlin, A. Boudaoud, E. Meyerowitz, Y. Couder and J. Traas, *Developmental patterning by mechanical signals in Arabidopsis*, Science **322** (2008) 1650–1655.
[3] F. Corson, O. Hamant, S. Bohn, J. Traas, A. Boudaoud and Y. Couder, *Turning a plant tissue into a living cell froth: a case of isotropic growth in plants*, Proceedings of National Academy of Sciences USA **106** (2009), 8453–8458.
[4] M. Uyttewaal, A. Burian, K. Alim, B. Landrein, D. Borowska-Wykret, A. Dedieu, A. Peaucelle, M. Ludynia, J. Traas, A. Boudaoud, D. Kwiatkowska and O. Hamant, *Mechanical Stress Acts via Katanin to Amplify Differences in Growth Rate between Adjacent Cells in Arabidopsis*, Cell **149** (2011), 439–451.
[5] K. Alim, O. Hamant and A. Boudaoud, *Regulatory role of cell division rules on tissue growth heterogeneity*, Frontiers in Plant Science **3** (2012),174.

The euglenoid movement in nature and for shape control of active surfaces

Marino Arroyo
(joint work with Antonio DeSimone)

Microorganisms swim in a viscous fluid without the help of inertia, and need to overcome the constraints imposed by the time-reversibility of Stokes equations. Their strategies, refined by evolution, can provide inspiration for artificial microfluidic devices such as micro-swimmers or pumps. While ciliary and flagellar locomotion have been extensively studied, the harmonious motility mode of euglenids, a family of protists, has remained a mystery in many aspects. These unicellular organisms, enclosed by a striated envelop composed of interlocking strips–the pellicle, move in a fluid by performing large amplitude, highly concerted shape changes. It is known that these changes are mediated by the relative sliding of the pellicle strips, i.e. a simple shear deformation of the cell surface along specified material lines.

Based on video recordings processed with machine learning techniques, we quantify the kinematics of this motility mode. Since movies report on shape changes but not on Lagrangian motions, we complete the observations with a kinematical model relating the local pellicle shear and the global geometry of the cell in order to obtain full velocity fields of the cell surface. This analysis establishes a clear link between biological actuation by molecular motors and shape changes, and allows us to estimate the hydrodynamic features of the movement of euglenids, which is slow but efficient when compared to flagellar motion [1].

With a view on engineering devices inspired on the movement of euglenids, we explore the attainable shapes starting from an ideal cylindrical pellicle [2]. Non-uniform pellicle shears create a target metric in the language of the theory of non-Euclidean plates, which may or may not be realized with an embedding of the deformed pellicle. We find it is possible to exactly realize a wide family of axisymmetric shapes, including cones, annular regions, or spherical and pseudo-spherical surface. We also understand the limits of embeddability. Numerically, we study

the behavior of thin active shells that try to realize target metrics beyond embeddability, and provide evidence for the flexibility of the actuation mode beyond axisymmetry.

References

[1] M. Arroyo, L. Heltai, D. Millan and A. DeSimone, *Reverse engineering the euglenoid movement*, Proceedings of the National Academy of Sciences USA **109** (2012), 17874–17879.

[2] M. Arroyo and A. DeSimone, *Shape control of active surfaces inspired by the movement of euglenids*, Journal of the Mechanics and Physics of Solids **62** (2014), 99–112.

Gradient structures and dissipation distances for reaction-diffusion systems

Alexander Mielke

(joint work with Matthias Liero, Giuseppe Savaré)

1. Gradient structures for reaction-diffusion systems

Looking at a reaction system with mass-action kinetics for a concentration vector $c = (c_1, .., c_I) \in]0, \infty[^I$ we obtain the ODE

$$\dot c = \mathbf{R}(c) = \sum_{r=1}^{R} \big(k^r_{\rm bw} c^{\beta^r} - k^r_{\rm fw} c^{\alpha^r}\big)\,(\alpha^r - \beta^r),$$

where $c^\gamma := \prod_{i=1}^I c_i^{\gamma_i}$ and $\alpha^r, \beta^r \in \mathbb{N}_0^I$ are the stoichiometric vectors associated to the rth reaction. The forward and the backward coefficients $k^r_{\rm fw}$ and $k^r_{\rm bw}$ are assumed to be positive.

The *detailed-balance condition* imposes the existence of a positive concentration vector $w \in]0, \infty[^I$ such that *all* reactions are individually balanced, i.e. $\kappa_r := k^r_{\rm fw} w^{\alpha^r} = k^r_{\rm bw} w^{\beta^r}$. It was shown in [Yon08, Mie11] that this condition allows us to write the reaction system $\dot c = \mathbf{R}(c)$ as an Onsager system, i.e.

$$\dot c = -\mathbb{K}_{\rm react}(c) {\rm D}F(c) \quad \text{with } F(c) = \sum_{i=1}^I w_i \beta(c_i/w_i) \text{ and } \beta(z) = z\log z - z + 1,$$

where the Onsager matrix $\mathbb{K}_{\rm react}(c) \in \mathbb{R}^{I\times I}$ is symmetric and positive semidefinite:

$$\mathbb{K}_{\rm react}(c) = \sum_{r=1}^{R} \kappa_r \Lambda\big(\tfrac{c^{\alpha^r}}{w^{\alpha^r}}, \tfrac{c^{\beta^r}}{w^{\beta^r}}\big)(\alpha^r - \beta^r) \otimes (\alpha^r - \beta^r) \quad \text{with } \Lambda(a,b) = \frac{a-b}{\log a - \log b}.$$

Thus, the reaction system can be understood as a gradient system (cf. [Mie13]) driven by the free energy (also called relative entropy of c with respect to w), since after restricting to suitable stoichiometric subspaces of $]0, \infty[^I$, we can invert $\mathbb{K}_{\rm react}$ and obtain the gradient flow $\mathbb{G}_{\rm react}(c)\dot c = -{\rm D}F(c)$.

According to [JKO98, Ott01] it is also possible to write diffusion equations as gradient flows with respect to the Wasserstein-Kantorovich metric. In [Mie11] this was generalized to reaction-diffusion systems satisfying the above detailed-balance

condition. Consider a bounded Lipschitz domain $\Omega \subset \mathbb{R}^d$ and density vectors $c(t,x) \in]0,\infty[^I$:

$$\dot c = \mathbf{D}\Delta c + R(c) = -\mathbb{K}_{\mathrm{RD}}(c)\mathrm{D}\mathcal{F}(c), \quad \text{where } \mathbf{D} = \mathrm{diag}(D_1,..,D_I), \tag{RDS}$$

with a total free energy $\mathcal{F}(c) = \int_\Omega F(c(x))\,\mathrm{d}x$ and an Onsager operator

$$\mathbb{K}_{\mathrm{RD}}(c) = \mathbb{K}_{\mathrm{diff}}(c) + \mathbb{K}_{\mathrm{react}}(c) \ \text{ with } \mathbb{K}_{\mathrm{diff}}(c)\xi := \big(-\mathrm{div}(D_i c_i \nabla \xi_i)\big)_{i=1,..,I}.$$

Here, the Onsager operator $\mathbb{K}_{\mathrm{RD}}$ is again symmetric and positive semidefinite. After a suitable restriction to invariant subspaces the Onsager operator $\mathbb{K}_{\mathrm{RD}}$ can be inverted to obtain an abstract metric tensor $\mathbb{G}_{\mathrm{RD}}(c) = \mathbb{K}_{\mathrm{RD}}(c)^{-1}$ and the gradient-flow form $\mathbb{G}_{\mathrm{RD}}(c)\dot c = -\mathrm{D}\mathcal{F}(c)$ of (RDS).

2. Dissipation distances

On the physical level one may introduce the primal and dual dissipation potentials Ψ and Ψ^*, where the latter is given in terms of $\mathbb{K}_{\mathrm{RD}}$ via $\Psi^*(c,\xi) :=$

$$\frac12\langle \xi, \mathbb{K}_{\mathrm{RD}}(c)\xi\rangle = \frac12\int_\Omega \sum_{i=1}^I D_i c_i |\nabla\xi_i|^2 + \sum_{r=1}^R \kappa_r \Lambda\big(\tfrac{c^{\alpha^r}}{w^{\alpha^r}}, \tfrac{c^{\beta^r}}{w^{\beta^r}}\big)\big((\alpha^r-\beta^r)\cdot\xi\big)^2\,\mathrm{d}x,$$

where we emphasize the additive structure in terms of the different dissipative mechanisms. Then, $\Psi(c,\dot c) := \frac12\langle \mathbb{G}_{\mathrm{RD}}(c)\dot c, \dot c\rangle$ is given by the Legendre-Fenchel transform of Ψ^* with respect to ξ, where the additive structure turns into a much more involved inf-convolution.

In some cases the formal infinitesimal metric $\mathbb{G}_{\mathrm{RD}}$ defines a so-called dissipation distance $D_{\mathrm{RD}} : L^1(\Omega;[0,\infty[^I) \times L^1(\Omega;[0,\infty[^I) \to [0,\infty]$ via

$$D_{\mathrm{RD}}(c_0,c_1)^2 := \inf\Big\{ \int_{s=0}^1 \langle \mathbb{G}_{\mathrm{RD}}(c)\dot c, \dot c\rangle\,\mathrm{d}s \;\Big|\; c(0)=c_0,\ c(1)=c_1,\ c \text{ smooth} \Big\}$$

Since $\mathbb{G}_{\mathrm{RD}}$ is only given implicitly, it is more advantageous to use the Benamou-Brenier formulation [BeB00] that is solely based on the Onsager operator, thus doing the inf-convolution implicitly, cf. [LiM13]:

$$D_{\mathrm{RD}}(c_0,c_1)^2 := \inf\Big\{ \int_{s=0}^1 \int_\Omega \Xi : \mathbb{D}(c)\Xi + \xi\cdot\mathbb{K}_{\mathrm{react}}(c)\xi\,\mathrm{d}x\,\mathrm{d}s \;\Big|\; c_0 \overset{c}{\rightsquigarrow} c_1,\ \dot c = \mathrm{div}(\mathbb{D}(c)\Xi) - \mathbb{K}_{\mathrm{react}}(c)\xi \Big\},$$

where the continuity equation $\dot c = \cdots$ now contains the classical transport term (cf. [AGS05]) as wells as the source term $\mathbb{K}_{\mathrm{react}}(c)\xi$ encoding the reactions.

The question of attainment of this infimum, which is the same as the existence of geodesic curves, is an open question in most cases. Nevertheless, in [LiM13] a differential theory of geodesically λ-convex functionals has been initiated as a generalization of the methods in [DaS08].

3. The Hellinger-Kantorovich distance

Motivated by the most simple scalar reaction-diffusion equation $\dot{u} = \Delta u - f(u)$, in [LMS14] we consider the Onsager operator

$$\mathbb{K}_{\mathrm{HK}}(u)\xi = -\alpha \mathrm{div}\big(u\nabla\xi\big) + \beta u\xi,$$

where α and β are nonnegative constants interpolating between the Wasserstein-Kantorovich distance (cf. [JKO98, AGS05]) for $(\alpha,\beta) = (1,0)$ and the Hellinger distance for $(\alpha,\beta) = (0,4)$, namely $D_{\mathrm{Hell}}(u_0,u_1)^2 = \int_\Omega \big(\sqrt{u_0(x)} - \sqrt{u_1(x)}\big)^2 \mathrm{d}x$.

For this special Onsager operator it is possible to show that it generates a true metric on the set of all nonnegative measures $\mathbb{M}_{\geq}(\overline{\Omega})$ on the underlying space Ω. The special choice of the above Onsager operator is its linearity in the state variable u. This allows us to consider curves of moving Dirac distributions. The squared length of the curve $\mu(s) = a(s)\delta_{x(s)}$ with $a(s) > 0$ and $x(s) \in \Omega$ can be calculated by the Benamou-Brenier formula as

$$\int_{s_0}^{s_1} \langle \mathbb{G}_{\mathrm{HK}}(\mu(s))\dot{\mu}'(s), \mu'(s)\rangle \,\mathrm{d}s = \int_{s_0}^{s_1} \frac{a(s)}{\alpha}|x'(s)|^2 + \frac{a'(s)^2}{\beta a(s)}\,\mathrm{d}s.$$

Thus, optimal transport between Dirac masses can be characterized: (i) For convex Ω the transport occurs along straight lines, but the speed is not constant. (ii) The mass $a(s)$ changes along the curve, even if $a(s_0) = a(s_1)$. (iii) There is a critical distance along which transport is no longer useful, so the initial mass $a(s_0)\delta_{x(s_0)}$ is destroyed (absorbed) at $x(s_0)$ while the final mass $a(s_1)\delta_{x(s_1)}$ is generated (desorbed) at $x(s_0)$. The latter effect follows from the fact that for large $|x(s_1)-x(s_0)|$ the functionals does not attain its infimum along a smooth curve.

In [LMS14] the Hellinger-Kantorovich distance D_{HK} is described as a function between any two positive measures in such a way that the competition between transport and reaction is clearly displayed. Moreover, we derive a characterization of the distance in terms of a minimization of a coupling measure and a cost function describing the transport part. The crucial point is to identify the amount of transport versus the amount of reaction.

References

[AGS05] L. Ambrosio, N. Gigli, and G. Savaré. *Gradient flows in metric spaces and in the space of probability measures*. Lectures in Mathematics ETH Zürich. Birkhäuser Verlag, Basel, 2005.

[BeB00] J.-D. Benamou and Y. Brenier. A computational fluid mechanics solution to the Monge-Kantorovich mass transfer problem. *Numer. Math.*, 84(3), 375–393, 2000.

[DaS08] S. Daneri and G. Savaré. Eulerian calculus for the displacement convexity in the Wasserstein distance. *SIAM J. Math. Analysis*, 40, 1104–1122, 2008.

[JKO98] R. Jordan, D. Kinderlehrer, and F. Otto. The variational formulation of the Fokker-Planck equation. *SIAM J. Math. Analysis*, 29(1), 1–17, 1998.

[LiM13] M. Liero and A. Mielke. Gradient structures and geodesic convexity for reaction-diffusion systems. *Phil. Trans. Royal Soc. A*, 371, 2013.

[LMS14] M. Liero, A. Mielke, and G. Savaré. Optimal transport in competition with reaction – the Hellinger–Kantorovich distance. *In preparation*, 2014.

[Mie11] A. Mielke. A gradient structure for reaction-diffusion systems and for energy-drift-diffusion systems. *Nonlinearity*, 24, 1329–1346, 2011.

[Mie13] A. Mielke. Thermomechanical modeling of energy-reaction-diffusion systems, including bulk-interface interactions. *Discr. Cont. Dynam. Systems Ser. S*, 6(2), 479–499, 2013.

[Ott01] F. Otto. The geometry of dissipative evolution equations: the porous medium equation. *Comm. Partial Differential Equations*, 26, 101–174, 2001.

[Yon08] W.-A. Yong. An interesting class of partial differential equations. *J. Math. Phys.*, 49, 033503, 21, 2008.

Hadamard's compatibility condition for microstructures

John Ball
(joint work with Carsten Carstensen)

The talk concerned generalizations of the Hadamard jump condition. The simplest version of this condition applies to a continuous piecewise C^1 map $y : \Omega \to \mathbb{R}^m$, where $\Omega \subset \mathbb{R}^n$ is open. If the gradient Dy jumps across a smooth surface through the point $a \in \Omega$ at which the normal to the surface is $N \in S^{n-1}$ then the limits $A = Dy^+(a)$, $B = Dy^-(a)$ of Dy at a from above and below the surface respectively are related by

$$A - B = b \otimes N \tag{1}$$

for some $b \in \mathbb{R}^m$. The generalizations are motivated by wanting to have a tool to help understand aspects of the complex patterns of microstructure resulting from solid phase transformations.

For an arbitrary locally Lipschitz map $y : \Omega \to \mathbb{R}^m$, a point $a \in \Omega$ and a unit vector $N \in S^{n-1}$, limiting sets of gradients $D^{+N}y(a)$ and $D^{-N}y(a)$ may be defined in terms of the gradient Young measures generated by $Dz^{(j)}$ on the unit ball $B(0,1)$ that are obtained by blowing up y around a using the formula

$$z^{(j)}(x) = \delta_j^{-1}(y(a + \delta_j x) - y(a)),$$

where $\delta_j \to 0$. Then one can prove the following results.

Theorem 2. *There exists $b \in \mathbb{R}^m$ such that*

$$b \otimes N \in [D^{+N}y(a)]^c - [D^{-N}y(a)]^c.$$

Here E^c denotes the convex hull of $E \subset M^{m\times n} = \{\text{real } \ m \times n \text{ matrices}\}$. This is a relatively easy result, valid for all dimensions m, n, and proved by a blow-up argument.

Theorem 3. *Let $m = n = 2$. There exists $b \in \mathbb{R}^2$ with*

$$b \otimes N \in [D^{-N}y(a)]^{pc} - [D^{+N}y(a)]^{pc}.$$

Here E^{pc} denotes the polyconvex hull of E. This is a more difficult result, whose proof uses the result that a Lipschitz map $u : B \to \mathbb{R}^n$, $B = B(0,1) \subset \mathbb{R}^n$ with $\det Du(x) \geq 1$ cannot vanish on the half-ball $B^- = \{x \in B(0,1) : x_n < 0\}$. This is a consequence of the result of Reshetnyak that a nonconstant quasiregular map is isolated (i.e. inverse images of points are isolated). A more elementary

proof of the lemma was given by Iwaniec, Verchota & Vogel [4], who also gave a counterexample to the theorem when $n = 2, m \geq 3$.

Similar results are valid for $W^{1,\infty}$ gradient Young measures, for which corresponding one-sided sets of gradients may be defined.

As an application of the second theorem we consider a bicrystal, in which there are two grains separated by a grain boundary whose normal is everywhere in the (x_1, x_2) plane. In the first grain the energy wells are given by

$$K = \mathrm{SO}(3)U_1 \cup \mathrm{SO}(3)U_2,$$

where $U_1 = \mathrm{diag}\,(\eta_2, \eta_1, \eta_1), U_2 = \mathrm{diag}\,(\eta_1, \eta_2, \eta_1)$ and $\eta_1 > 0, \eta_2 > 0$, while the axes of crystallization in the second grain are rotated about the vertical x_3 axis through an angle α, so that the energy wells are

$$KR_\alpha = \mathrm{SO}(3)U_1R_\alpha \cup \mathrm{SO}(3)U_2R_\alpha,$$

where R_α is the rotation. A minimum-energy microstructure then corresponds to a gradient Young measure $(\nu_x)_{x\in\Omega}$ with $\mathrm{supp}\,\nu_x \in K$ a.e. in grain 1, and $\mathrm{supp}\,\nu_x \in KR_\alpha$ a.e. in grain 2. It is always possible to have minimum-energy microstructure in both grains with $Dy = \bar{\nu}_x = (\eta_1^2\eta_2)^{1/3}\mathbf{1}$. We aim to prove that it is impossible to have a minimum-energy microstructure which is a pure phase in one of the grains, i.e. $\nu_x = \delta_A$ in one of the grains for some matrix A. In fact, if the interface is planar, then whatever its orientation there always exists a zero-energy microstructure which has a pure phase in one of the grains. So one needs a curved interface to prevent this. As an example, suppose that $\alpha = \pi/4$. Then it is impossible to have a zero-energy microstructure with a pure phase in one of the grains if the interface contains a normal $(\cos\theta, \sin\theta) \in D_1$ and another normal $(\cos\theta', \sin\theta') \in D_2$, where

$$D_1 = (\frac{\pi}{8}, \frac{3\pi}{8}) \cup (\frac{5\pi}{8}, \frac{7\pi}{8}) \cup (\frac{9\pi}{8}, \frac{11\pi}{8}) \cup (\frac{13\pi}{8}, \frac{15\pi}{8}),$$

$$D_2 = (\frac{-\pi}{8}, \frac{\pi}{8}) \cup (\frac{3\pi}{8}, \frac{5\pi}{8}) \cup (\frac{7\pi}{8}, \frac{9\pi}{8}) \cup (\frac{11\pi}{8}, \frac{13\pi}{8}).$$

The proofs of these statements use:

1. A reduction to the case $m = n = 2$ using the plane strain result for the two-well problem [2].
2. The characterization of the quasiconvex hull of two wells [3], which equals their polyconvex hull.
3. Use of the generalized Hadamard jump condition to show that there has to be a rank-one connection $b \otimes N$ between the polyconvex hulls for each grain.
4. Long and detailed calculations.

The results described here will appear in [1].

References

[1] J.M. Ball and C. Carstensen. Hadamard's compatibility condition for microstructures. In preparation.

[2] J.M. Ball and R.D. James. A characterization of plane strain. *Proc. Roy. Soc. London A*, 432:93–99, 1991.

[3] J.M. Ball and R.D. James. Proposed experimental tests of a theory of fine microstructure, and the two-well problem. *Phil. Trans. Roy. Soc. London A*, 338:389–450, 1992.
[4] T. Iwaniec, G.C. Verchota, and A.L. Vogel. The failure of rank-one connections. *Arch. Ration. Mech. Anal.*, 163:125–169, 2002.

Buckling of axially compressed circular cylindrical shells

Yury Grabovsky
(joint work with Davit Harutyunyan)

Axially compressed cylindrical shells will buckle producing a variety of buckling patterns[2, 7, 3]. For example, soda cans buckle with an audible click, accompanied by an appearance of a diamond-shaped dimple and an abrupt drop in load [6]. The dimple disappears upon unloading. This suggests that the observed phenomenon is purely elastic. Shell theoretic analysis [8, 9] results in the critical buckling stress

$$\sigma_{\text{crit}} = \frac{Eh}{\sqrt{3(1-\nu^2)}}, \qquad h = \frac{t}{R}, \tag{1}$$

where t and R are the wall thickness and the radius of the circular cylindrical shell, respectively. The conundrum is that the experimentally observed critical stress does not agree with the above formula in two important ways. One, is that the predicted critical stress is 4 to 5 times larger than the experimental, the other, is that the critical stress scales as $h^{1.5}$ [10] in direct contradiction to (1). There is a general agreement that the buckling load of axially compressed cylindrical shells exhibits high sensitivity to imperfections. However, a complete theoretical understanding of mechanisms of this behavior is lacking. Generically, imperfections eliminate sharp bifurcation transitions [1]. However, the abrupt character of the observed buckling of soda cans, with visible dents, suggests that, in the case of cylindrical shells, shape imperfections *do not eliminate bifurcation instability*. If this is indeed the case, the rigorous theory of buckling of slender structures [5] would be applicable.

Let $\Omega_h \subset \mathbb{R}^3$ be a slender body, characterized by the slenderness parameter h. The energy of the loaded body is given by

$$\mathcal{E}(\boldsymbol{u}) = \int_{\Omega_h} W(\nabla \boldsymbol{u}) d\boldsymbol{x} - \int_{\partial\Omega_h} \boldsymbol{t}_h(\boldsymbol{x};\lambda)\cdot \boldsymbol{u} dS(\boldsymbol{x}),$$

where λ plays the role of the loading parameter. The displacement $\boldsymbol{u}$ must also be constrained in order to avoid flip instability [5]. Most linear constraints on $\boldsymbol{u}$ can be described in terms of a given "Dirichlet data" function $\overline{\boldsymbol{u}}_h(\boldsymbol{x};\lambda)$ and a subspace

$$W_0^{1,\infty}(\Omega_h;\mathbb{R}^3) \subset V_h^0 \subset W^{1,\infty}(\Omega_h;\mathbb{R}^3),$$

so that $\boldsymbol{u} \in \overline{\boldsymbol{u}}_h(\boldsymbol{x};\lambda) + V_h^0$. We assume that the trivial branch $\boldsymbol{u}(\boldsymbol{x};\lambda,h)$ is a Lipschitz equilibrium of $\mathcal{E}(\boldsymbol{u})$, such that $\nabla \boldsymbol{u}(\boldsymbol{x};h,\lambda) = \lambda \nabla \boldsymbol{u}_h(\boldsymbol{x}) + o(\lambda)$ in L^∞, uniformly in h, where $\boldsymbol{u}_h$ solves a system of equations of linear elasticity:

$$\nabla\cdot(\mathsf{L}_0 e(\boldsymbol{u}_h)) = 0, \quad \mathsf{L}_0 = W_{\boldsymbol{HH}}(\boldsymbol{0}), \quad e(\boldsymbol{u}) = \frac{1}{2}(\nabla \boldsymbol{u} + (\nabla \boldsymbol{u})^T).$$

We identify the onset of buckling with the smallest value of λ for which the second variation of energy

$$\delta^2\mathcal{E}(\boldsymbol{\phi}) = \int_{\Omega_h} (W_{\boldsymbol{HH}}(\nabla \boldsymbol{u}(\boldsymbol{x}; h, \lambda))\nabla\boldsymbol{\phi}(\boldsymbol{x}), \nabla\boldsymbol{\phi}(\boldsymbol{x}))d\boldsymbol{x}$$

can be made negative for some $\boldsymbol{\phi} \in V_h = \overline{V_h^0} \subset W^{1,2}(\Omega_h; \mathbb{R}^3)$:

$$\lambda_{\text{crit}}(h) = \inf\{\lambda > 0 : \delta^2\mathcal{E}(\boldsymbol{\phi}) < 0 \text{ for some } \boldsymbol{\phi} \in V_h\}.$$

The goal is to determine the asymptotics of $\lambda_{\text{crit}}(h) \to 0$, as $h \to 0$. The idea in [5] is that for small values of λ, the local *material* response is linearly elastic. The global non-linearity is of purely geometric nature. Thus, the material response can be linearized, while preserving the full geometric non-linearity. This process of constitutive linearization leads to the "linearized" second variation

$$\delta^2\mathcal{E}_{cl}(\boldsymbol{\phi}) \sim \int_{\Omega_h} \left\{ (\mathsf{L}_0 e(\boldsymbol{\phi}), e(\boldsymbol{\phi})) + \frac{\lambda}{4}\widetilde{\boldsymbol{\sigma}}_h \nabla \times \boldsymbol{\phi} \cdot \nabla \times \boldsymbol{\phi} \right\} d\boldsymbol{x},$$

where

$$\widetilde{\boldsymbol{\sigma}}_h = (\operatorname{Tr} \boldsymbol{\sigma}_h)\boldsymbol{I} - \boldsymbol{\sigma}_h, \qquad \boldsymbol{\sigma}_h(\boldsymbol{x}) = \mathsf{L}_0 e(\boldsymbol{u}_h).$$

Replacing $\delta^2\mathcal{E}$ with $\delta^2\mathcal{E}_{cl}$ leads to the "constitutively linearized critical load"

$$\widehat{\lambda}(h) = \inf_{\boldsymbol{\phi}\in\mathcal{A}_h} \frac{-4\int_{\Omega_h}(\mathsf{L}_0 e(\boldsymbol{\phi}), e(\boldsymbol{\phi}))d\boldsymbol{x}}{\int_{\Omega_h} \widetilde{\boldsymbol{\sigma}}_h \nabla \times \boldsymbol{\phi} \cdot \nabla \times \boldsymbol{\phi} d\boldsymbol{x}},$$

$$\mathcal{A}_h = \left\{ \boldsymbol{\phi} \in V_h : \int_{\Omega_h} \widetilde{\boldsymbol{\sigma}}_h \nabla \times \boldsymbol{\phi} \cdot \nabla \times \boldsymbol{\phi} d\boldsymbol{x} < 0 \right\}.$$

Theorem. Suppose that

$$\lim_{h\to 0} K(V_h) = 0, \qquad \lim_{h\to 0} \frac{\widehat{\lambda}(h)^2}{K(V_h)} = 0.$$

Then $\lambda_{\text{crit}}(h)/\widehat{\lambda}(h) \to 1$, as $h \to 0$. Here

$$K(V_h) = \inf_{\boldsymbol{\phi}\in V_h} \frac{\|e(\boldsymbol{\phi})\|^2}{\|\nabla\boldsymbol{\phi}\|^2}$$

is the Korn constant of the loaded slender structure. In fact we *define* the structure to be slender if $K(V_h) \to 0$, as $h \to 0$. The theorem establishes the asymptotics of the critical load in terms of the linearly elastic stress $\boldsymbol{\sigma}_h$.

For the circular cylindrical shell we have

$$V_h = \{\boldsymbol{\phi} \in W^{1,2}(\mathcal{C}_h; \mathbb{R}^3) : \phi_\theta(r, \theta, 0) = \phi_z(r, \theta, 0) = \phi_\theta(r, \theta, L) = \phi_z(r, \theta, L) = 0\}.$$

where the cylindrical coordinate system is used. In [4] we show that the ansatz

$$\begin{cases} \phi_r^h(r,\theta,z) = & -W_{,\eta\eta}\left(\frac{\theta}{\sqrt[4]{h}}, z\right) \\ \phi_\theta^h(r,\theta,z) = & r\sqrt[4]{h}W_{,\eta}\left(\frac{\theta}{\sqrt[4]{h}}, z\right) + \frac{r-1}{\sqrt[4]{h}}W_{,\eta\eta\eta}\left(\frac{\theta}{\sqrt[4]{h}}, z\right), \\ \phi_z^h(r,\theta,z) = & (r-1)W_{,\eta\eta z}\left(\frac{\theta}{\sqrt[4]{h}}, z\right) - \sqrt{h}W_{,z}\left(\frac{\theta}{\sqrt[4]{h}}, z\right), \end{cases}$$

achieving the optimal scaling in the Korn inequality $K(V_h) = O(h^{3/2})$, also achieves optimal scaling in the Korn-like inequalites for gradient components:

$$(2) \quad \frac{\|e(\boldsymbol{\phi}^h)\|^2}{\|(\nabla \boldsymbol{\phi}^h)_{r\theta}\|^2} = O(h^{3/2}), \quad \frac{\|e(\boldsymbol{\phi}^h)\|^2}{\|(\nabla \phi^h)_{\theta,z}\|^2} = O(\sqrt{h}), \quad \frac{\|e(\boldsymbol{\phi}^h)\|^2}{\|(\nabla \phi^h)_{r,z}\|^2} = O(h).$$

The 3 distinct scaling exponents in (2) are the key to our explanation of the paradoxical scaling of the critical stress in experiments. For the perfect shell we find that $\boldsymbol{\sigma}_h = -\boldsymbol{e}_z \otimes \boldsymbol{e}_z$, and hence, $\lambda(h) \sim Ch$. *Generic* order ϵ imperfections of load result in $\boldsymbol{\sigma}_h \to -\boldsymbol{e}_z \otimes \boldsymbol{e}_z + \epsilon \boldsymbol{e}_\theta \otimes \boldsymbol{e}_z + \epsilon \boldsymbol{e}_z \otimes \boldsymbol{e}_\theta$, which leads to

$$\widehat{\lambda}(h) \sim \frac{Ch^{5/4}}{\epsilon + h^{1/4}}.$$

Regarding the load imperfection characteristic ϵ a constant, while $h \to 0$, we conclude that load imperfections cause the critical stress scaling law instability, whereby the exponent of h jumps from the classical value of 1 to 5/4. However, in practice, it is unlikely that $\epsilon \gg h^{1/4}$, so the imperfections of load alone cannot be responsible for the observed values and scaling of the critical stress.

Our technical results for circular cylindrical shells cannot be immediately applied to an "imperfectly shaped" shell. Heuristically, however, we may observe that the structure of $\boldsymbol{\sigma}_h$ is in large part determined by the condition that the lateral surfaces are stress-free. A very small dint described, for example by

$$\mathcal{C}_h^\epsilon = \left\{ 1 + \epsilon\rho\left(\frac{\theta}{\sqrt{\epsilon}}, \frac{z}{\sqrt{\epsilon}}\right) - \frac{h}{2} \le r \le 1 + \epsilon\rho\left(\frac{\theta}{\sqrt{\epsilon}}, \frac{z}{\sqrt{\epsilon}}\right) + \frac{h}{2} \right\},$$

changes the surface normal by a finite amount on a small set. This leads to the stress

$$\boldsymbol{\sigma}_h = -\boldsymbol{e}_z \otimes \boldsymbol{e}_z - \rho_{,zz} \boldsymbol{e}_\theta \otimes \boldsymbol{e}_\theta + O(\sqrt{\epsilon}),$$

and $\widehat{\lambda}(h) \sim h^{3/2}$. This argument is in some sense similar to the arguments in [10], where the estimates of elastic energy stored in a small dimple lead to $h^{3/2}$ scaling of the critical stress.

References

[1] B. Budiansky and J. Hutchinson. A survey of some buckling problems. Technical Report CR-66071, NASA, February 1966.

[2] D. Bushnell. Buckling of shells-pitfall for designers. *AIAA J*, 19(9):1183–1226, 1981.

[3] R. Degenhardt, A. Kling, R. Zimmermann, F. Odermann, and F. de Araújo. Dealing with imperfection sensitivity of composite structures prone to buckling. In S. B. Coskun, editor, *Advances in Computational Stability Analysis*. InTech, 2012.

[4] Y. Grabovsky and D. Harutyunyan. Exact scaling exponents in korn and korn-type inequalities for cylindrical shells. submitted.

[5] Y. Grabovsky and L. Truskinovsky. The flip side of buckling. *Cont. Mech. Thermodyn.*, 19(3-4):211–243, 2007.

[6] J. Griggs. Experimental study of buckling of thin-walled cylindrical shells. Masters of arts thesis, Temple University, Philadelphia, PA, May 2010.

[7] E. Lancaster, C. Calladine, and S. Palmer. Paradoxical buckling behaviour of a thin cylindrical shell under axial compression. *International Journal of Mechanical Sciences*, 42(5):843 – 865, 2000.

[8] R. Lorenz. Die nicht achsensymmetrische knickung dünnwandiger hohlzylinder. *Physikalische Zeitschrift*, 12(7):241–260, 1911.
[9] S. Timoshenko and S. Woinowsky-Krieger. *Theory of plates and shells*, volume 2. McGraw-hill New York, second edition, 1959.
[10] E. Zhu, P. Mandal, and C. Calladine. Buckling of thin cylindrical shells: an attempt to resolve a paradox. *International Journal of Mechanical Sciences*, 44(8):1583 – 1601, 2002.

Energy-driven pattern formation via competing long- and short-range interactions

Florian Theil
(joint work with David Bourne, Mark Peletier)

We prove strong crystallization results in two dimensions for an energy that arises in the theory of block copolymers. The energy is defined on sets of points and their weights, or equivalently on the set of atomic measures. It consists of two terms; the first term is the sum of the square root of the weights, and the second is the quadratic optimal transport cost between the atomic measure and the Lebesgue measure.

We prove that this system admits crystallization in several different ways: (1) the energy is bounded from below by the energy of a triangular lattice (called $\mathcal{T}$); (2) when the energy equals that of $\mathcal{T}$, then the measure is a rotated and translated copy of $\mathcal{T}$; (3) when the energy is close to that of $\mathcal{T}$, then the measure is close to a rotated and translated copy of $\mathcal{T}$. These three results require the domain to be a polygon with at most six sides. A fourth result states that the energy of $\mathcal{T}$ can be achieved in the limit of large domains, for domains with arbitrary boundaries.

The proofs make use of three ingredients. First, the optimal transport cost associates to each point a polygonal *cell*; the energy can be bounded from below by a sum over all cells of a function that depends only on the cell. Second, this function has a convex lower bound that is sharp at $\mathcal{T}$. Third, Euler's polytope formula limits the average number of sides of the polygonal cells to six, where six is the number corresponding to the triangular lattice.

References

[1] D. Bourne, M. Peletier & F. Theil. *Optimality of the triangular lattice for a particle system with Wasserstein interaction.* To appear in Comm. Math. Phys., arxiv.org/abs/1212.6973.

Optimal Scaling in Ductile Fracture

Michael Ortiz
(joint work with Sergio Conti, Landry Fokoua)

Regularized energy functions with sublinear growth have recently been proposed as models for ductile fracture [1, 2]. To date, the connection between such functionals and fracture properties has been limited to optimal scaling. Specifically, the aim is to derive optimal scaling laws, in the sense of matching lower and upper

bounds on the energy, for a solid undergoing ductile fracture. The specific problem considered by Fokoua *it al.* [1, 2] concerns a material sample in the form of an infinite slab of finite thickness subjected to prescribed opening displacements on its two surfaces. The solid is assumed to be incompressible and to obey deformation-theory of plasticity. The problem is thus reduced to the minimization of energies of the form

$$E(y) = \int_\Omega W(Dy, D^2y)\, dx \tag{1}$$

over volume-preserving deformation mappings $y : \Omega \to \mathbb{R}^3$. When hardening exponents are given values consistent with observation, $W(\cdot, D^2y)$ is found to exhibit sublinear growth. The additional dependence of W on the second gradient D^2y represents a regularization of the strain-gradient plasticity type. This nonlocal regularization has the effect of introducing an intrinsic length scale ℓ into the energy. An appeal to dislocation mechanics then reveals that $W(Dy, \cdot)$ has linear growth. These considerations justify the growth assumptions

$$\begin{aligned} &C_L \int_\Omega (|Dy|^p - 3^{p/2})dx + \ell \int_\Omega |DDy|\, dx \le E(y) \le \\ &C_U \int_\Omega (|Dy|^p - 3^{p/2})dx + \ell \int_\Omega |DDy|\, dx, \end{aligned} \tag{2}$$

with $p \in (0, 1)$ and constants $C_U > C_L > 0$. Under these assumptions, ductile fracture indeed emerges as the net result of two competing effects: whereas the sublinear growth of the local energy promotes localization of deformation to failure planes, the nonlocal regularization stabilizes this process, thus resulting in an orderly progression towards failure and a well-defined specific fracture energy. Specifically, for a slab of area L^2 and thickness H subjected to opening displacements δ we have [1, 2],

$$c_L(p) L^2 \ell^{\frac{1-p}{2-p}} \delta^{\frac{1}{2-p}} \le E_{\min} \le c_U(p) L^2 \ell^{\frac{1-p}{2-p}} \delta^{\frac{1}{2-p}}, \tag{3}$$

for suitable constants c_L and c_U depending only on the growth exponent p and independent of the thickness H. The upper bound follows by construction, e. g., by localization of deformations to *void sheets*. The optimal scaling laws show that the energy scales with L^2 and, therefore, that ductile fracture requires a well-defined energy per unit fracture area. In particular, fractal modes of fracture are ruled out under the assumptions of the analysis. The optimal scaling laws additionally show that ductile fracture is cohesive in nature, i. e., it obeys a well-defined relation between energy and opening displacement δ. Finally, the scaling laws supply a link between micromechanical properties and macroscopic fracture properties. In particular, they shed light on the relative roles that strain-gradient plasticity and microplasticity play as contributors to the specific fracture energy of the material.

References

[1] Fokoua, L., Conti, S. and Ortiz, M., *Optimal scaling in solids undergoing ductile fracture by void sheet formation*, Archive for Rational Mechanics and Analysis (2014) in press.

[2] Fokoua, L., Conti, S. and Ortiz, M., *Optimal scaling laws for ductile fracture derived from strain-gradient microplasticity*, Journal of the Mechanics and Physics of Solids, **62** (2014), 295–311.

Closure and commutability results for Gamma-limits and an application to multi-well energy functionals

Bernd Schmidt
(joint work with Martin Jesenko)

We report on a recent closure and commutability result for Gamma-limits and an application to the simultaneous geometric linearization and homogenization of multi-well energy functionals, cf. [5]. Our abstract theorem gives a new perspective to some older problems that

(1) identifies a general scheme which is behind:
- the homogenization of almost periodic functionals (Braides 1986, [1]),
- the passage from nonlinear to linear elasticity (Dal Maso/Negri/Percivale 2002, [2]),
- the passage from nonlinear to geometrically linear elasticity for multi-well energies (Schmidt 2008, [7]),
- the commutability of homogenization and linearization (Müller/Neukamm 2011, [6], and Gloria/Neukamm 2011, [4])

(2) and also allows for new applications, e.g.:
- a proof of the commutability of homogenization and geometric linearization of multi-well energies,
- numerical schemes for multiscale problems (future work).

Let $U \subset \Omega \subset \mathbb{R}^n$ be open and bounded sets with Lipschitz boundary. We consider a doubly indexed family of Borel functions $f_\varepsilon^{(j)} : \Omega \times \mathbb{R}^{m\times n} \to \mathbb{R}$ satisfying a uniform growth assumption of the form

$$-\beta \le f_\varepsilon^{(j)}(x, X) \le \beta(|X|^p + 1),$$

where $j \nearrow \infty$ and $\varepsilon \searrow 0$. We set

$$F_\varepsilon^{(j)}(u, U) = \begin{cases} \int_U f_\varepsilon^{(j)}(x, \nabla u(x))\, dx, & u \in W^{1,p}(\Omega; \mathbb{R}^m), \\ +\infty & \text{otherwise,} \end{cases}$$

and simply write $F_\varepsilon^{(j)}$ for $F_\varepsilon^{(j)}(\cdot, \Omega)$. In addition we assume that the $F_\varepsilon^{(j)}(\cdot, U)$ satisfy a 'Gårding type inequality' of the form:

$$F_\varepsilon^{(j)}(u, U) \ge \alpha_U \int_\Omega |\nabla u|^p - \gamma_U \int_\Omega |u|^p$$

for suitable constants $\alpha_U > 0$, $\gamma_U \in \mathbb{R}$.

Theorem 1. (Γ-closure for Gårding type functionals.) Suppose that

(i) For each $j < \infty$ the Γ-limit $\Gamma\text{-}\lim_{\varepsilon\to 0} F_\varepsilon^{(j)} =: F_0^{(j)}$ exists.

(ii) The families $((f_\varepsilon^{(j)})_{\varepsilon>0})_{j\in\mathbb{N}}$ and $(f_\varepsilon^{(\infty)})_{\varepsilon>0}$ are equivalent on Ω in the sense that

$$\lim_{j\to\infty} \limsup_{\varepsilon\to 0} \int_\Omega \sup_{|X|\le R} |f_\varepsilon^{(j)}(x,X) - f_\varepsilon^{(\infty)}(x,X)|\,dx = 0$$

for every $R \ge 0$.

Then also $\Gamma\text{-}\lim_{\varepsilon\to 0} F_\varepsilon^{(\infty)} =: F_0^{(\infty)}$ exists and is the pointwise and the Γ-limit of $F_0^{(j)}$ as $j\to\infty$:

$$F_0^{(\infty)} = \lim_{j\to\infty} F_0^{(j)} = \Gamma\text{-}\lim_{j\to\infty} F_0^{(j)}.$$

$$\begin{array}{ccc} F_\varepsilon^{(j)} & \overset{\approx}{=\!=} & F_\varepsilon^{(\infty)} \\ \Gamma\big\downarrow & & \big\downarrow\Gamma \\ F_0^{(j)} & \xrightarrow{\Gamma,\ \text{ptw.}} & F_0^{(\infty)} \end{array}$$

Corollary 2. (Localized Γ-closure for Gårding type functionals.) Suppose that the assumptions of Theorem 1 are satisfied for each $U \subset \Omega$ open, bounded with Lipschitz boundary. Then the limiting functionals for $j \in \mathbb{N}\cup\{\infty\}$ are given by unique densities $f_0^{(j)}$ and in addition to the previous assertions we have

$$f_0^{(j)}(\cdot,X) \overset{*}{\rightharpoonup} f_0^{(\infty)}(\cdot,X) \quad \text{in } L^\infty(\Omega)$$

for all $X \in \mathbb{R}^{m\times n}$.

Remarks.

(1) Theorem 1 and Corollary 2 extend Braides' homogenization closure theorem (cf. [1]) by
- allowing for generally x- and ε-dependent densities $f_\varepsilon^{(j)}(x,X)$ rather than $f^{(j)}(\frac{x}{\varepsilon},X)$ and
- dropping the quasiconvexity assumption and
- relaxing the lower growth condition on the densities.

The last two points are crucial for our application to frame indifferent elastic energy densities with multiple wells to be discussed below.

(2) There is always a subsequence such that $\Gamma\text{-}\lim_{\varepsilon\to 0} F_\varepsilon^{(j)}(\cdot,U)$ exists for all j, U.

(3) The upper bound on the densities simplifies the proof but is in fact not necessary.

Another direct consequence of Theorem 1 is that, under a slightly stronger notion of equivalence which in particular is satisfied if '$\limsup_\varepsilon$' can be replaced by '$\sup_\varepsilon$', the limits $\varepsilon\to 0$ and $j\to\infty$ commute:

Corollary 3. (Commutability.) Suppose that in addition to the assumptions of Theorem 1 for every $\varepsilon > 0$ and $R > 0$

$$\lim_{j\to\infty} \int_\Omega \sup_{|X|\le R} |f_\varepsilon^{(j)}(x,X) - f_\varepsilon^{(\infty)}(x,X)|\,dx = 0.$$

If $\operatorname{lsc} F_\varepsilon^{(\infty)}$ denotes the lower semicontinuous envelope of $F_\varepsilon^{(\infty)}$, then the following diagram commutes:

$$\begin{array}{ccc} F_\varepsilon^{(j)} & \xrightarrow{\Gamma} & \operatorname{lsc} F_\varepsilon^{(\infty)} \\ \Gamma \downarrow & & \downarrow \Gamma \\ F_0^{(j)} & \xrightarrow{\Gamma} & F_0^{(\infty)} \end{array}$$

Our main application is given by rescaled energy functionals of elastic materials with

$$f_\varepsilon^{(j)}(x, X) = \delta^{-2} W_\delta(\tfrac{x}{\varepsilon}, \mathrm{Id} + \delta X),$$

where W_δ is the stored energy function and $\varepsilon, \delta = \delta_j > 0$ are small. The $\frac{x}{\varepsilon}$-dependence accounts for highly oscillating material mixtures typically leading to microstructures. The explicit and implicit δ-dependence allows for modelling energy densities with multiple wells that are separated by a distance which is comparable to the size of deformation gradients δX that may thus explore multiple wells. Under suitable assumptions on W_δ (see [5]) we observe that the geometric rigidity result of Friesecke, James and Müller [3] implies that such functionals satisfy our assumptions and, in particular, are of Gårding type.

Remarks.

(1) In the special case of $f_\varepsilon^{(j)}$ being independent of ε we recover the Γ-convergence results of nonlinear to linear elasticity theory from [2] (for a single well density $W_\delta = W$) and on geometric linearization from [7] (for multiple wells).

(2) For densities W with a non-degenerate single well we obtain the results on commutability of linearization and homogenization from [6] and [4].

In fact, our abstract Theorem 1 and Corollaries 2 and 3 also apply to multiple energy wells. As a result, we obtain that also for such systems (periodic or stochastic) homogenization and geometric linearization commute.

For a more complete discussion of our results and all proofs we refer to [5].

References

[1] A. Braides, *A homogenization theorem for weakly almost periodic functionals*, Rend. Accad. Naz. Sci. XL **104** (1986), 261–281.

[2] G. Dal Maso, M. Negri, D. Percivale, D, *Linearized elasticity as Γ-limit of finite elasticity*, Set-Valued Anal. **10** (2002), 165–183.

[3] G. Friesecke, R. James, S. Müller, *A theorem on geometric rigidity and the derivation of nonlinear plate theory from three-dimensional elasticity*, Comm. Pure Appl. Math. **55** (2002), 1461–1506.

[4] A. Gloria, S. Neukamm, *Commutability of homogenization and linearization at identity in finite elasticity and applications*, Ann. Inst. H. Poincaré AnalN̈on Linéaire **28** (2011), 941–964.

[5] M. Jesenko, B. Schmidt, *Closure and commutability results for Gamma-limits and an application to multi-well energy functionals*, arXiv-Preprint arXiv:1308:0963v1, submitted 2013.

[6] S. Müller, S. Neukamm, *On the commutability of homogenization and linearization in finite elasticity*, Arch. Ration. Mech. Anal. **201** (2011), 465–500.

[7] B. Schmidt, *Linear Γ-limits of multiwell energies in nonlinear elasticity theory*, Contin. Mech. Thermodyn. **20** (2008), 375–396.

Periodic Homogenization in Elasto-Plasticity

Gilles A. Francfort
(joint work with Alessandro Giacomini)

We propose to report on our investigation [3] of the interplay between periodic homogenization and quasi-static elasto-plasticity.

The setting is that of small strain perfect elasto-plasticity. The N-dimensional unit cell (or unit torus) Y is made up of p elasto-plastic disjoint phases, Y_i, $i = 1, ..., p$, each characterized by a Hooke's law, denoted by A_i, and by a set of admissible stresses (a yield criterion), K_i (a convex, compact subset of trace-free symmetric matrices containing 0). For simplicity sake, we assume that A_i and K_i remain constant throughout Y_i. We also assume that ∂Y_i is piecewise C^2. We then define $A(y)$ and $K(y)$ in an obvious way, and for any given $\varepsilon > 0$, we set

$$A_\varepsilon(x) := A(x/\varepsilon),\ K_\varepsilon := K(x/\varepsilon).$$

Then, for a (bounded, Lipschitz, open, connected) domain $\Omega \subset \mathbb{R}^N$, we propose to investigate the following problem:

$$\mathrm{div}\sigma_\varepsilon(t) = 0 \text{ in } \Omega, \quad \sigma_\varepsilon(t)\nu = 0 \text{ on } \partial\Omega \setminus \bar{\Gamma}_d, \qquad \text{(equilibrium)}$$

$$(\sigma_\varepsilon)_D(t) \in K_\varepsilon \text{ a.e. in } \Omega, \qquad \text{(stress admissibility)}$$

$$\dot{p}_\varepsilon(t) \in \partial I_{K_\varepsilon}((\sigma_\varepsilon)_D(t)) \text{ a.e. in } \Omega, \qquad \text{(flow rule).}$$

where, a.e. in Ω,

$$\sigma_\varepsilon(t) = A_\varepsilon e_\varepsilon(t) \qquad \text{(constitutive law).}$$

Above, Γ_d (a relatively open subset of $\partial\Omega$) is the Dirichlet part of the boundary $\partial\Omega$ while the notation σ_D stands for the deviatoric (trace-free) part of the stress field σ. Further I_K denotes the indicatrix function of K. Finally, e_ε and p_ε (a trace-free matrix) are such that, for some time-dependent (displacement) field $u_\varepsilon(t) : \Omega \to \mathbb{R}^N$,

$$Eu_\varepsilon(t) := \frac{\nabla u_\varepsilon(t) + \nabla u_\varepsilon^T(t)}{2} = e_\varepsilon(t) + p_\varepsilon(t).$$

The system above is completed by appropriate initial conditions that will not be detailed here, as well as by the boundary condition

$$u_\varepsilon(t) = w(t) \text{ on } \Gamma_d.$$

Under appropriate regularity assumptions on w and on the relative boundary of Γ_d, we had shown in prior work [2] that such a system has, roughly speaking, a solution

$$(u_\varepsilon, e_\varepsilon, p_\varepsilon) \in AC(0, T; BD(\Omega) \times L^2(\Omega; \mathbb{R}^{N\times N}_{sym}) \times \mathcal{M}_b(\Omega \cup \Gamma_d; \mathbb{R}^{N\times N}_{sym})),$$

(the symbol $\mathcal{M}_b$ standing for "bounded Radon measure"), provided that the boundary condition is relaxed to

$$p_\varepsilon(t) = (w(t) - u_\varepsilon(t)) \odot \nu \text{ on } \Gamma_d,$$

ν being the exterior normal to $\partial\Omega$ at the point under consideration.

In [3], we propose to pass to the limit as ε, the size of the microstructure, goes to 0. To this effect, we appeal to two-scale convergence which has to be tailored to the kinematic structure of the elasto-plastic setting. In a nutshell, we establish the existence of a two-scale limit evolution to the ε-problem in the form

$$(u, E, P) \in AC(0,T; BD(\Omega) \times L^2(\Omega \times Y; \mathbb{R}^{N\times N}_{sym}) \times \mathcal{M}_b((\Omega \cup \Gamma_d) \times Y; \mathbb{R}^{N\times N}_{sym})),$$

that satisfies a two-scale kinematic compatibility condition, namely,

$$E(x,y,t)\,(\mathcal{L}^N_x \otimes \mathcal{L}^N_y) + P - Eu \otimes \mathcal{L}^N_y = E_y\mu,$$

with

$$\mu \in \big\{\pi \in \mathcal{M}_b((\Omega \cup \Gamma_d) \times Y; \mathbb{R}^N)) : E_y\pi \in \mathcal{M}_b((\Omega \cup \Gamma_d) \times Y; \mathbb{R}^{N\times N}_{sym});$$
$$\pi(F \times Y) = 0 \text{ for every Borel set } F \subseteq \Omega \cup \Gamma_d\big\}.$$

Further, setting $\Sigma(x,y,t) := A(y)E(x,y,t)$, the triplet also satisfies two-scale equilibrium and stress admissibility in the form

$$\mathrm{div}_y\Sigma = 0 \quad \text{on } \Omega \times Y, \qquad \Sigma_D(t) \in K(y) \quad \text{a.e. in } \Omega \times Y$$

and

$$\mathrm{div}_x\sigma = 0 \text{ in } \Omega, \quad \sigma \cdot \nu = 0 \text{ on } \partial\Omega \setminus \overline{\Gamma}_d,$$

where $\sigma(x) := \int_Y \Sigma(x,y)\,dy$.

Finally, the following flow rules are satisfied for a.e. x in Ω:

$$\frac{\dot P_x(t)}{|\dot P_x(t)|}(y) \in N_{K(y)}(\Sigma_D(t,x,y)) \qquad \text{for } \mathcal{L}^N_y \text{ a.e. } y \in \{|\dot P_x(t)| > 0\},$$

where $\dot P_x$ is such that the disintegration of $\dot P$ with respect to the measure $\eta := \mathcal{L}^N_x + (proj_\#|P|)^s$ ($proj$ denoting the projection of $(\Omega\cup\Gamma_d)\times Y$ on the first factor, and $proj_\#$ the associated push forward of measures) reads as

$$\dot P = \eta \otimes \dot P_x;$$

see e.g. [1, Theorem 2.28]. (There are also interfacial and boundary flow rules that we choose not to detail in this abstract).

The above system cannot be reduced to a system in the sole variables (x,t), in contrast with what is usually the case for a two-scale convergence result.

The extent to which the resulting system exhibits an "elasto-plastic type" behavior is unclear to us because the obtained flow rules on $P(x,y,t)$ are equations in the y-variable and thus view $P(x,\cdot,\cdot)$ as an (infinite) list of internal variables parameterized by the physical point x, whereas, thermo-mechanically, one should think of an (infinite) list of internal variables $P(\cdot,y,\cdot)$ parameterized by the texture y, this resulting in a flow rule in x for a.e. $y \in Y$. Unfortunately, it is not possible to switch the disintegration around and to obtain such a structure for the flow rules.

References

[1] L. Ambrosio, N. Fusco, Nicola and D. Pallara, *Functions of Bounded Variation and Free Discontinuity Problems*, Oxford University Press, 2000.
[2] G.A. Francfort and A.. Giacomini, *Small Strain Heterogeneous Elasto-Plasticity Revisited*, Comm. Pure Appl. Math. **65**,9 (2012), 1185–1241.
[3] G.A. Francfort and A.. Giacomini, *On periodic homogenization in perfect plasticity*, J. Eur. Math. Soc., to appear.

Non-Riemannian geometries and the nonlinear mechanics of distributed defects

Arash Yavari
(joint work with Alain Goriely)

Many interesting properties of solids are controlled by defects and their evolution. The study of line defects in solids goes back to the work of Volterra [1] more than a century ago. The close connection between the mechanics of solids with distributed defects and non-Riemannian geometries was independently discovered in the 1950s by Kondo [2, 3] and Bilby [4, 5]. These works while seminal and very interesting were mostly kinematic in nature. This has also been the case for the more recent works based on the ideas of Kondo and Bilby. In other words, no stress calculations have been reported to this date based on these geometric ideas. Defects induce residual stresses and one problem of interest in the mechanics of defects is to calculate these stresses. To date, stress calculations for defective solids are overwhelmingly restricted to linear elasticity.

Recently we introduced a geometric framework in which one can analytically calculate the stress field of nonlinear solids with distributed line and point defects. The idea is to find a manifold (material manifold) in which the body is stress free by construction. In other words, the nonlinear mechanics of solids with distributed defects can be formulated as a nonlinear elasticity problem provided that the material manifold – where the body is stress-free – is chosen appropriately. If one can find such a manifold then the problem of residual stress calculation is simply to find an embedding of the material manifold into the Euclidean ambient space. We have used this geometric framework for calculating the stress fields of nonlinear solids with distributed dislocations [6], disclinations [7], and point defects [8].

In [6] we presented a comprehensive theory of the mechanics of distributed dislocations based on Riemann-Cartan geometry. We showed that in the geometric framework several examples of residual stress fields of solids with distributed dislocations can be solved analytically. In this work the machinery of Cartan's moving frames [9, 10] were used to construct the material manifold. In the case of distributed dislocations we work with a Weitzenböck manifold (a manifold with a flat and metric-compatible affine connection that has non-vanishing torsion). The torsion tensor is identified with the given dislocation density tensor. We have also discussed the geometric meaning of "lack of closure" in a Burger's closed path using the idea of curve development in differential geometry [11].

Later in [7], we extended the geometric theory to the mechanics of solids with distributed disclinations. Here the curvature 2-form is given and one can construct the Riemannian material manifold using Cartan's structural equations.

The residual stress field of a single point defect in an infinite linear elastic solid has a $1/r^3$ singularity and was obtained by Love [12] almost ninety years ago. Interestingly, there has not been any nonlinear solutions for single or distributed point defects in the literature. In [8], we calculated the residual stress field of a nonlinear elastic solid with a spherically-symmetric distribution of point defects. The material manifold is a flat Weyl manifold, i.e., a manifold with an affine connection that has non-metricity but both its torsion and curvature tensors vanish. Given a spherically-symmetric point defect distribution, we constructed its Weyl material manifold using the method of Cartan's moving frames. In the case of arbitrary incompressible solids we calculated the residual stress field. We also compared the nonlinear and classical linear solutions and showed that they agree in the limit of a single point defect with small strength.

References

[1] Volterra, V., Sur l'équilibre des corps élastiques multiplement connexes. *Annales Scientifiques de l'Ecole Normale Supérieure, Paris* **24**(3), 1907:401-518.

[2] Kondo, K. 1955, Geometry of elastic deformation and incompatibility, *Memoirs of the Unifying Study of the Basic Problems in Engineering Science by Means of Geometry*, (K. Kondo, ed.), vol. 1, Division C, Gakujutsu Bunken Fukyo-Kai, 1955, pp. 5-17.

[3] Kondo, K. 1955, Non-Riemannian geometry of imperfect crystals from a macroscopic viewpoint, *Memoirs of the Unifying Study of the Basic Problems in Engineering Science by Means of Geometry*, (K. Kondo, ed.), vol. 1, Division D-I, Gakujutsu Bunken Fukyo-Kai, 1955, pp. 6-17.

[4] Bilby, B. A., R., Bullough, and E., Smith 1955, Continuous distributions of dislocations: a new application of the methods of non-Riemannian geometry. *Proceedings of the Royal Society of London* **A231**(1185):263-273.

[5] Bilby, B. A., and E., Smith 1956, Continuous distributions of dislocations. III. *Proceedings of the Royal Society of London* **A236**(1207): 481-505.

[6] Yavari, A. and A. Goriely, Riemann-Cartan geometry of nonlinear dislocation mechanics, *Archive for Rational Mechanics and Analysis* **205**(1), 2012, pp. 59-118.

[7] Yavari, A. and A. Goriely, Riemann-Cartan geometry of nonlinear disclination mechanics, *Mathematics and Mechanics of Solids* **18**(1), 2013, pp. 91-102.

[8] Yavari, A. and A. Goriely, Weyl geometry and the nonlinear mechanics of distributed point defects, *Proceedings of the Royal Society A* **468**, 2012, pp. 3902-3922.

[9] Cartan, E., Sur les variétés a connexion affine et la théorie de la relativité généralisée (premiére partie suite). *Annales Scientifiques de lÉcole Normale Superieure* **41**, 1924:1-25.

[10] Cartan, E., *On Manifolds with an Affine Connection and the Theory of General Relativity*. Bibliopolis, Napoli, 1955.

[11] Ozakin, A. and A. Yavari, Affine development of closed curves in Weitzenböck manifolds and the Burgers vector of dislocation mechanics, *Mathematics and Mechanics of Solids*, 10.1177/1081286512463720.

[12] Love, A.H. 1927, *Mathematical Theory of Elasticity*. Cambridge University Press, Cambridge.

The effect of the unloading response on the necking of elastic bars

Basile Audoly
(joint work with John W. Hutchinson)

We consider the stretching of a slender rectangular solid by an imposed displacement applied at its ends. By using a deformation theory (a nonlinear elasticity theory which mimics plasticity as long as stretch increases monotonically), we assume a fictitious material which under tensile stretch, like most ductile metals, has a force-elongation relation for which the force attains a maximum at a stretch λ_{m} and then decreases. For slender geometries, it is well known that homogeneous solutions become unstable slightly past the maximum stretch [2, 4], and that the post-buckling behavior can be described by a second-gradient bar model [1, 3]. This classical theory of elastic necking predicts a discontinuous transition (snap-back) as necked solutions arise through a discontinuous pitchfork bifurcation. We observe, however, that outside the neck in which the stretch continues to increase, the stretch begins to decreases along the bifurcated branch. This makes the deformation theory constitutive model inapplicable to metals because as soon as the stretch begins to decrease a metal displays an abrupt and large increase in incremental stiffness known as linear elastic unloading. We argue that a realistic model of unloading must involve a new parameter, the tangent unloading modulus K. We show that this parameter has a strong effect on the global load-displacement curve: when K is large enough, necked solutions appear through a *continuous* bifurcation. By contrast with the prediction of the classical theory of necking based on the nonlinear elastic constitutive model, we show that it is possible to observe the gradual necking of an initially homogeneous bar when controlling the displacement of its ends.

References

[1] B. D. Coleman and D. C. Newman. On the rheology of cold drawing. I. elastic materials. *Journal of Polymer Science: Part B: Polymer Physics*, 26:1801–1822, 1988.

[2] R. Hill and J. W. Hutchinson. Bifurcation phenomena in the plane tension test. *Journal of the Mechanics and Physics of Solids*, 23(4–5):239–264, 1975.

[3] A. Mielke. *Hamiltionian and Lagrangian flows on center manifolds, with application to elliptic variational problems*, volume 1489 of *Lecture notes in mathematics*. Springer-Verlag, 1991.

[4] W. Scherzinger and N. Triantafyllidis. Asymptotic analysis of stability for prismatic solids under axial loads. *Journal of the Mechanics and Physics of Solids*, 46(6):955–1007, 1998.

Do optimal thin rods contain homogenized regions?

Guy Bouchitté
(joint work with J.J Alibert, I.Fragalà, I.Lucardesi)

Let $\varphi : \mathbb{R}^2 \to \mathbb{R}$ be the following convex but non-strictly convex integrand:

$$\varphi(y) := \begin{cases} \frac{|y|^2}{2} + \frac{1}{2} & \text{if } |y| \geq 1 \\ |y| & \text{if } |y| < 1\,. \end{cases} \tag{1}$$

Let D be a Jordan domain in $\mathbb{R}^2$ and let s be a real parameter. We consider the convex variational problem

$$m(s) := \inf \left\{ \int_{\mathbf{R}^2} \varphi(\nabla u) \ : \ u \in H^1_0(D)\,,\ \int_{\mathbf{R}^2} u = s \right\}, \tag{2}$$

for which existence of solutions is quite classical. We say that u is a *special solution* to $m(s)$ if it minimizes (2) and satisfies

$$|\nabla u| \in \{0\} \ \cup \ (1, +\infty\,) \text{ a.e. in } D\ .$$

We are interested in the following question:

$$\textit{Does problem } m(s) \textit{ admit a special solution?} \tag{3}$$

This question, which was raised in [2], appears as an important issue in the context of shape optimization of thin torsion rods. The mechanical motivation is developed in [1] where the optimal compliance of an elastic structure disposed in a thin design domain subject to an external load is studied within a framework of a 3D-2D reduction analysis. In [3] the case of a thin cylindric design (of cross section D) subject to a torsion load is considered and we refer to this paper for enlighting the precise meaning of problem (2) and the choice of the non quadratic integrand φ given in (1). In this context, question (3) corresponds to ask whether or not an optimal configuration should contain some homogenization region, that is made of a finely perforated material. If a special solution exists, then the minimal compliance is obtained when the elastic material occupies the subset $\{|\nabla u| > 1\}$. To our knowledge, there is no rigorous counterexample to the existence of a special solution (that is to the existence of an optimal shape) although there is numerical evidence in the case of a square as shown at the end of this report.

Below we adopt the following notation: if u is a special solution to problem $m(s)$, we call the *plateau* of u, and we denote it by $\Omega(u)$, the set $\{\nabla u = 0\}$. The set $\Gamma(u) := \partial\Omega(u) \cap D$ will be called the *free boundary* of u (see Figure 1).

Our main results concern the study of question (3) in relation with the geometry of the domain D and also with the value of the parameter s. They are listed hereafter:

• If u is a minimizer to (2) for $s > 0$, then $u \geq 0$ and the "upper plateau" $\{u = \|u\|_\infty\}$ has positive measure. Futhermore the function $m(s)$ is convex differentiable

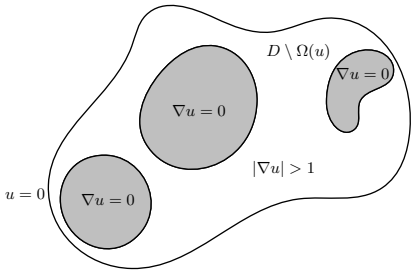

FIGURE 1. *Behaviour of special solutions.*

on $(0, +\infty)$ and the slope of m at zero satisfies $m'(0^+) = h_D$ being h_D the Cheeger constant of D, that is

$$h_D := \inf_{A \subset \overline{D}} \frac{|\partial A|}{|A|} = \inf \left\{ \int_D |\nabla v| \ : \ v \in BV(\mathbb{R}^2), \ \int_D v = 1, v = 0 \text{ in } \mathbb{R}^2 \setminus \overline{D} \right\}.$$

• When D is a ball or a ring, through explicit computations and exploiting the optimality conditions, we show that $m(s)$ admits a special solution, and there is no other solution. For an explicit expression of this radial solution we refer also to [6] for more general integrands.

• *Gradient constraint free boundary problem.* Let $s > 0$ and $\lambda = m'(s)$. Assume that we can find a plateau $\Omega \subset D$ smooth enough such that

(1) $h_\Omega = \lambda$ and $\frac{|\partial\Omega|}{|\Omega|} = h_\Omega$ (Ω is then Cheeger set of itself).
(2) There exits a solution $u \in H_0^1(D)$ to the *overdetermined* problem

$$\begin{cases} -\triangle u = h_\Omega \quad , \quad |\nabla u| > 1 & \text{in } D \setminus \Omega \\ |\nabla u| = 1 & \text{on } \partial\Omega \\ u \text{ constant on each connected part of} & \partial\Omega \end{cases}$$

Then u is the (unique) special solution to problem $m(s)$.

• Balls and rings are *not* the unique domains for which $m(s)$ admits a special solution. In this respect, it is worth to compare our results with those obtained by Murat and Tartar in [5], about the problem of maximizing the torsional rigidity of a bar with a given cross-section made by two linearly elastic materials in fixed proportions. The corresponding variational problem is quite similar to ours, except that it involves a *differentiable* integrand, and classical solutions (*i.e.* optimal designs with no homogenization regions) cannot exist unless the cross-section D is a disk. In our case the integrand φ is non-differentiable at zero and the conclusion goes in a quite opposite direction: we prove that there exists a non circular domain D with analytic boundary such that, for some s, problem $m(s)$ admits a special solution. Moreover this solution has a convex plateau with analytic boundary.

• *Uniqueness.* By using comparison arguments we show that the solution to (2) is unique provided parameter s ranges in an intervall (s_1, s_2) where $m(s)$ is stricly

convex. On the opposite way, if $m(s)$ is affine on such interval, then no special solution can exist.

• Assuming that D is simply connected, and that there exists a special solution u with a smooth free boundary,

- we prove that each connected component of $D \setminus \Omega(u)$ must touch ∂D,
- by using the theory of P-functions and Hopf's Lemma, we prove that if D is convex and if the plateau $\Omega(u)$ is smooth and compactly supported in D, then $\Omega(u)$ is convex,
- we show that, when D is not Cheeger set of itself, the plateau $\Omega(u)$ cannot be compactly contained into D for arbitrarily small filling ratios.

We point out that characterizing domains D where a special solution to $m(s)$ exists seems to be a very challenging problem, which remains by now open: in this respect we believe that, at least when D is convex, the existence of special solutions is likely related to the regularity of ∂D, and also to whether or not D coincides with its Cheeger set. Let us notice that the latter criterium would exclude the existence of a special solution in the case when D is a square. This guess, that we try to prove by using recents results on shape derivatives (see [4]), seems to be confirmed by the numerical results performed C. Galusinski [7], in which homogenization regions are observed for small values of parameter s (square and slender ellipse).

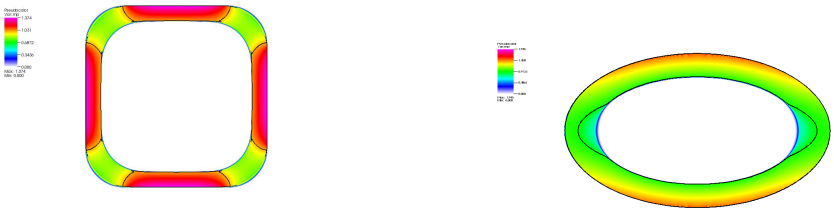

[red or yellow zone $|\nabla u| > 1$, green zones $0 < |\nabla u| < 1$, white: $\nabla u = 0$]

References

[1] G.Bouchitté, I.Fragalà, P.Seppecher *Structural optimization of thin elastic plates: the three dimensional approach*, Arch. Rat. Mech. Anal., 202 **3** (2011), 829–874.

[2] G.Bouchitté, I.Fragalà, I.Lucardesi, P.Seppecher *Optimal Thin Torsion Rods and Cheeger Sets*, SIAM J. Math. Anal. 44 **1** (2012), 483 –512.

[3] J.J Alibert, G.Bouchitté, I.Fragalà, I.Lucardesi *A nonstandard free boundary problem arising in the shape optimization of thin torsion rods*, Interfaces and Free Boundaries, 15 (2013) **1**, 95–119

[4] G.Bouchitté, I.Fragalà, I.Lucardesi *Shape derivatives for minima of integral functionals*, Mathematical Programming, (2014)

[5] F. Murat, L. Tartar *Calcul des variations et homogénéisation* Homogenization methods: theory and applications in physics (Bráu-sans-Nappe, 1983), 319-369, Collect. Dir. Etudes Rech. Elec. France **5**, Eyrolles, Paris (1985).

[6] A. Cellina, *Uniqueness and comparison results for functionals depending on ∇u and on u*, SIAM J. Control Optim., 18 (2007), 711–716.

[7] C. Galusinski, private communication

Metastability and dynamics of discrete topological singularities via Gamma-convergence: Application to dislocations

Adriana Garroni
(joint work with Roberto Alicandro, Lucia De Luca, Marcello Ponsiglione)

Our goal is to study the metastability and the dynamics for a system of discrete screw dislocations in a lattice. In doing this we exploit the strict relation between the discrete models for dislocations and the modeling of vortices in spin systems.

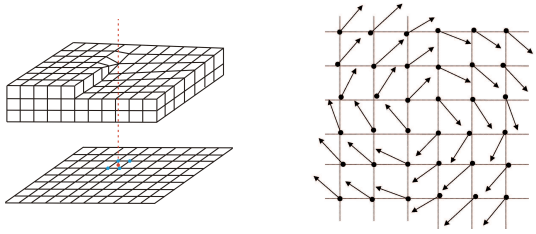

Figure 1. A screw dislocation versus a vortex in spin systems

As a prototype model for screw dislocations we consider the elastic energy defined on the scalar discrete (scaled) vertical displacement $u : \varepsilon\mathbb{Z}^2 \cap \Omega \to \mathbb{R}$ given by

$$SD_\varepsilon(u) := \frac{1}{2} \sum_{i,j \in \varepsilon\mathbb{Z}^2 \cap \Omega \ , \ |i-j|=\varepsilon} \mathrm{dist}^2(u(i) - u(j), \mathbb{Z}),$$

where $\varepsilon\mathbb{Z}^2 \cap \Omega$ represents the two dimensional projection of a cylindrical cubic crystal. The periodicity of the energy is consistent with the fact that plastic deformations, corresponding to integer jumps of u, do not store elastic energy, according with Nabarro Peierls and Frenkel Kontorova theories [12]. This type of potentials are commonly used in models for dislocations (see e.g. [11], [15]; see also [8] for more general discrete lattice energies accounting for defects).

Another celebrated model, which allows to describe the formation of topological singularities, as vortices in superconductors, is the so-called XY model for spin systems. Here, the order parameter is a vectorial spin field $v : \varepsilon\mathbb{Z}^2 \cap \Omega \to \mathcal{S}^1$ and the corresponding energy is given by

$$XY_\varepsilon(v) := \frac{1}{2} \sum_{i,j \in \varepsilon\mathbb{Z}^2 \cap \Omega \ \ |i-j|=\varepsilon} |v(i) - v(j)|^2.$$

Notice that $XY_\varepsilon(v)$ can be written in terms of a representative of the phase of v, defined as a scalar field u such that $v = e^{2\pi i u}$. In this respect, both models can be regarded as specific examples of scalar systems governed by periodic potentials f acting on first neighbors, whose energy is of the type

$$F_\varepsilon(u) := \sum_{i,j \in \varepsilon\mathbb{Z}^2 \cap \Omega \ , \ |i-j|=\varepsilon} f(u(i) - u(j)).$$

A typical vortex singularity for the XY-system is represented by the function $\frac{x}{|x|}$ and the corresponding phase can be seeing as a configuration which represents a screw dislocation. We characterize the defects for these systems in terms of a notion of discrete topological degree for the field $v = e^{2\pi i u}$; they are point singularities, and can be identified by the discrete vorticity measure $\mu(u)$. This is a finite sum of Dirac masses centered in the squares of the lattice, and with multiplicities equal to either $+1$ or -1. This notion in the case of dislocations corresponds to the discrete circulation of the plastic strain, and $\mu(u)$ represents the Nye dislocation density.

The first step in our analysis is the asymptotic expansion in terms of Γ-convergence ([7], [10]) of the discrete energies F_ε, as $\varepsilon \to 0$. This analysis relies on the powerful machinery developed in the recent past for the analysis of Ginzburg-Landau functionals, which can be somehow considered the continuous counterpart of the energies F_ε (see [16] and the references therein, and [5]).

Each singularity carries a quantum of energy of order $|\log \varepsilon|$, and this can be seen by studying the Γ-limit of the energies F_ε scaled by $|\log \varepsilon|$ ([14], [1], [2]). For these Γ-convergence results, the relevant variable is the vorticity measure $\mu(u)$ and the topology should take into account that many dipoles are compatible with a logarithmic energy bound. Therefore, the compactness of the vorticity measures fails in the usual sense of weak star convergence, while it can be proved in the flat topology, which, roughly speaking, measures the shortest connections between positive and negative masses.

In order to see the interaction between singularities, we remove the leading term from the energy and we study the next order Γ-limit. We show that, given $M \in \mathbb{N}$, the functionals $F_\varepsilon(u) - M\pi|\log \varepsilon|$ Γ-converge to $\mathbb{W}(\mu) + M\gamma$, where μ is a sum of M singularities x_i with degrees $d_i = \pm 1$. Here $\mathbb{W}$ is the renormalized energy as in the Ginzburg-Landau setting, defined by

$$\mathbb{W}(\mu) := -\pi \sum_{i \neq j} d_i d_j \log |x_i - x_j| - \pi \sum_i d_i R_0(x_i),$$

where R_0 is a suitable harmonic function, and γ can be viewed as a core energy, depending on the specific discrete interaction energy.

As a consequence of our Γ-convergence analysis, we show that F_ε has many local minimizers. Precisely, we show that, under suitable assumptions on the potential f, given any configuration of singularities $x \in \Omega^M$, there exists a stable configuration $\tilde{x}$ at a distance of order ε from x. Starting from these configurations, the gradient flow of F_ε is clearly stuck. These results are proven for a general class of energies, including SD_ε, while the case of the XY_ε energy, to our knowledge, is still open. A similar analysis of stable configurations in the triangular lattice has been recently carried on in [13], using different technics.

In order to study the discrete dynamics, we propose a simple variational mechanism, following the minimizing movements approach à la De Giorgi ([6], [9]), that permits to overcome the barriers and that accounts for the slip directions in the crystals. We discretize time by introducing a time scale $\tau > 0$, and at each time

step we minimize a total energy, which is given by the sum of the free energy plus a dissipation.

The choice of the dissipation is done taking into account that a dislocation, in order to move from one cell to a neighboring one, should overcome an energy barrier and then the energy paid in moving a dislocation is proportional to the number of horizontal and vertical bonds that separate the initial and the final configuration. In other words it is proportional to the distance between the initial and the final configuration, measured in the Manhattan metric. Precisely we introduce the Wasserstein distance between two positive measures μ and ν as

$$2\text{-}W_1(\mu,\nu) = \inf_{\lambda\in\Pi(\mu,\nu)} \int_{\overline{\Omega}\times\overline{\Omega}} |x-y|_1^2 d\lambda(x,y)\,,$$

where $|x-y|_1 = |x^1-y^1|+|x^2-y^2|$ is the Manhattan distance in $\mathbb{R}^2$ and $\Pi(\mu,\nu)$ denotes the set of measures defined in $\overline{\Omega}\times\overline{\Omega}$ whose marginals in Ω are respectively μ and ν. With this definition the dissipation between two vorticity measures μ and ν, both sums of Dirac masses with positive and negative weights, is given by

$$D_2(\mu,\nu) = 2\text{-}W_1(\mu^+ + \nu^-, \nu^+ + \mu^-)\,.$$

We fix an initial condition $\mu_0 := \sum_{i=1}^M b_{i,0}\delta_{x_{i,0}}$ with $|b_{i,0}| = 1$ and a sequence of "well prepared" initial conditions $\mu_{\varepsilon,0}$. We introduce the energy $E_\varepsilon(\mu)$ obtained by minimizing the energy $F_\varepsilon(u)$ among all functions with vorticity given by μ. Then, given $\delta > 0$ and a time step $\tau > 0$, we construct iteratively $\mu_k^{\tau,\varepsilon} = \sum_i b_{i,0}\delta_{x_{i,k}^{\tau,\varepsilon}}$ as the minimum point of

$$\min\left\{ E_\varepsilon(\mu) + \frac{1}{2\tau} D_2(\mu, \mu_{k-1}^{\tau,\varepsilon}) \;:\; \|\mu - \mu_{k-1}^{\tau,\varepsilon}\|_{flat} \le \delta \right\}$$

with $\mu_0^{\tau,\varepsilon} = \mu_{\varepsilon,0}$. Since the renormalized energy is not bounded for below, in the step by step minimization we are led to consider local rather than global minimizers. Precisely, we minimize the energy in a δ neighborhood of the minimizer at the previous step. Without this care, already at the first step we would have, in the limit as $\varepsilon \to 0$, the trivial solution $\mu = 0$, corresponding to the fact that dipoles annihilate and the remaining singularities reach the boundary of the domain. Nevertheless, for τ small the minimizers do not touch the constraint, so that they are in fact true local minimizers.

For any fixed τ, we refer to this process as *discrete gradient flow*. It turns out that, during the step by step energy minimization, the singularities are able to overcome the energy barriers, that are of order ε. Therefore, taking the limit as $\varepsilon \to 0$ and then as $\tau \to 0$ the solutions $\mu_k^{\tau,\varepsilon}$ of the discrete gradient flow converge to $\mu(t) = \sum_i b_{i,0}\delta_{x_i(t)}$, where the trajectories $x_i(t)$, with $i = 1,\dots,M$, are solutions of the following differential inclusion

$$\dot{x_i} \in \partial^- G(-\nabla_{x_i} W(x_1,\dots,x_M))\,,$$

where

$$G(\xi) = \sum_{i=1}^M \max\{|\xi_i^1|, |\xi_i^2|\}$$

and $\xi = ((\xi_1^1, \xi_1^2), \dots, (\xi_M^1, \xi_M^2)) \in \mathbb{R}^{2M}$. Note that in general the two components of the gradient of the renormalized energy will not agree and then the differential inclusion rewrites as a differential equation that allows the motion only in one of the two coordinate directions. In other words we have deduced a continuous in time dynamics that account for glide directions as a consequence of the dissipations distance chosen in the discrete dynamics. The above results can be found in [3] and [4].

References

[1] Alicandro R., Cicalese M.: *Variational Analysis of the Asymptotics of the XY Model*, Arch. Ration. Mech. Anal., **192** (2009) no. 3, 501–536.

[2] Alicandro R., Cicalese M., Ponsiglione M.: *Variational equivalence between Ginzburg- Landau, XY spin systems and screw dislocations energies*, Indiana Univ. Math. J., no. 1, 171–208.

[3] Alicandro R., De Luca L., Garroni A., Ponsiglione M.: *Metastability and dynamics of discrete topological singularities in two dimensions: a* Γ*-convergence approach*, Arch. Ration. Mech. Anal., to appear.

[4] Alicandro R., De Luca L., Garroni A., Ponsiglione M.: *Dynamics for discrete screw dislocations accounting for glide directions*, in preparation.

[5] Alicandro R., Ponsiglione M.: *Ginzburg-Landau functionals and renormalized energy: A revised* Γ*-convergence approach*, Preprint 2011.

[6] Ambrosio L., Gigli N., Savaré G.: *Gradient flows in metric spaces and in the space of probability measures*. Second edition, Lectures in Mathematics ETH Zürich. Birkhäuser Verlag, Basel, 2008.

[7] Anzellotti G., Baldo S.: *Asymptotic development by* Γ*-convergence*, Appl. Math. Optim. **27** (1993), no. 2, 105–123.

[8] Ariza, M. P.; Ortiz, M.: *Discrete crystal elasticity and discrete dislocations in crystals*, Arch. Ration. Mech. Anal. **178** (2005), no. 2, 149–226.

[9] Braides A.: *Local minimization, variational evolution and* Γ*-convergence*, Lecture Notes in Mathematics, Springer, Berlin, to appear.

[10] Braides A., Truskinovsky L.: *Asymptotic expansions by* Γ*-convergence*, Contin. Mech. Thermodyn. **20** (2008), no. 1, 21–62.

[11] Celli V. , Flytzanis N.: *Motion of a Screw Dislocation in a Crystal*, J. of Appl. Phys., **41** 11 (1970), 4443–4447.

[12] Hirth J.P., Lothe J.: *Theory of Dislocations*, Krieger Publishing Company, Malabar, Florida, 1982.

[13] Hudson T., Ortner C.: *Existence and stability of a screw dislocation under anti-plane deformation*, Preprint (2013).

[14] Ponsiglione M.: *Elastic energy stored in a crystal induced by screw dislocations: from discrete to continuous*, SIAM J. Math. Anal. **39** (2007), no. 2, 449–469.

[15] Salman O.U., Truskinovsky L.: *On the critical nature of plastic flow: One and two dimensional models*, Internat. J. of Engin. Sc. **59** (2012), 219–254.

[16] Sandier E., Serfaty S.: *Vortices in the Magnetic Ginzburg-Landau Model*, Progress in Nonlinear Differential Equations and Their Applications, vol. 70, Birkhäuser Boston, Boston (MA), 2007.

Lattice Point Problems and the Surface Energy of Crystals

Phoebus Rosakis

We investigate some connections between the continuum and atomistic descriptions of deformable crystals, using certain interesting results from number theory.

The energy of a deformed crystal is calculated in the context of a lattice model with binary interactions (pair potentials) in two dimensions. A new bond counting approach is used, which reduces the problem to the lattice point problem of number theory. When the crystal shape is a lattice polygon (the convex hull of lattice points), we show that the energy due to a homogeneous deformation equals the bulk elastic energy, plus the boundary integral of a surface energy density, plus the sum over the vertices of a corner energy function. This is an exact result when the interatomic potential has finite (but otherwise arbitrary) range; for infinite-range potentials it is asymptotically valid as the lattice parameter approaches zero. The surface energy density is obtained explicitly as a function of the deformation gradient and the boundary unit normal. The corner energy is found as an explicit function of the deformation gradient and the normals of the two facets meeting at the corner.

For more general convex domains with possibly curved boundary, the surface energy density depends on the unit normal in a striking way. It is continuous at irrational directions, discontinuous at rational ones and nowhere differentiable. This pathology is alarming since it may render the Wulff surface energy minimization problem (under domain variations) ill-posed. An alternative approach of defining the continuum region containing the crystal is introduced, that restores continuity of the surface energy density function. These results have been reported in [1]. The generalization to three dimensions is standard.

We also present preliminary results which furnish a remarkably simple explicit representation of the interfacial energy density of phase boundaries and twin interfaces, modeled as piecewise-affine deformations of the crystal.

References

[1] P. Rosakis, *Continuum Surface Energy from a Lattice Model* , arXiv:1201.0712

Reporter: Manh Hong Duong, Patrick van Meurs

Participants

Virginia Agostiniani
Mathematical Institute
Oxford University
Woodstock Road
Oxford OX1 3LB
UNITED KINGDOM

Prof. Dr. Hans Wilhelm Alt
Zentrum Mathematik
TU München
Arcisstr. 21
80333 München
GERMANY

Prof. Dr. Marino Arroyo
Universitat Politecnica de
Catalunya (UPC)
Jordi Girona 1-3
08034 Barcelona
SPAIN

Dr. Basile Audoly
Institut Jean le Rond d'Alembert
Université Pierre & Marie Curie
Paris VI, Case 162
4, place Jussieu
75252 Paris CEDEX 05
FRANCE

Prof. John M. Ball
Mathematical Institute
Oxford University
Andrew Wiles Building
Woodstock Rd
Oxford OX2 6GG
UNITED KINGDOM

Prof. Dr. Davide Bigoni
Dipartimento di Ingegneria Meccanica
e Strutturale
University of Trento
Via Mesiano, 77
38050 Trento
ITALY

Prof. Dr. Guy Bouchitté
U.F.R. des Sc. et Techn.
Université de Toulon et du Var
B.P. 132
83957 La Garde Cedex
FRANCE

Dr. Arezki Boudaoud
Département de Physique
École Normale Superieure
24, rue Lhomond
75231 Paris Cedex 05
FRANCE

Prof. Dr. Yann Brenier
CMLS
École Polytechnique
Plateau de Palaiseau
91128 Palaiseau Cedex
FRANCE

Giancarlo Cicconofri
S.I.S.S.A.
Via Bonomea 265
34136 Trieste
ITALY

Prof. Dr. Eric Clement
PMMH-ESPCI
10, rue Vauquelin
75231 Paris Cedex 5
FRANCE

Prof. Dr. Antonio DeSimone
SISSA
Via Bonomea 265
34136 Trieste
ITALY

Lukas Doering
Max-Planck-Institut für Mathematik
in den Naturwissenschaften
04103 Leipzig
GERMANY

Dr. Patrick W. Dondl
Dept. of Mathematical Sciences
Durham University
Science Laboratories
South Road
Durham DH1 3LE
UNITED KINGDOM

Manh Hong Duong
Department of Mathematics
Eindhoven University of Technology
P.O.Box 513
5600 MB Eindhoven
NETHERLANDS

Prof. Dr. Gilles Francfort
393 4th Street
Apt. 4
Brooklyn NY 11215
UNITED STATES

Prof. Dr. Adriana Garroni
Dipartimento di Matematica
"Guido Castelnuovo"
Universita di Roma "La Sapienza"
Piazzale Aldo Moro, 2
00185 Roma
ITALY

Prof. Dr. Dmitry Golovaty
Department of Mathematical Sciences
University of Akron
Akron, OH 44325-4002
UNITED STATES

Prof. Dr. Yury Grabovsky
Department of Mathematics
Temple University
Philadelphia, PA 19122
UNITED STATES

Dr. Georgy Kitavtsev
Max-Planck-Institut für Mathematik
in den Naturwissenschaften
Inselstr. 22 - 26
04103 Leipzig
GERMANY

Prof. Dr. Martin Kruzik
Inst. of Info. Theory & Automation
Academy of Sciences of the Czech R.
Pod Vodarenskou vezi 4
P.O.Box 18
182 08 Prague 8
CZECH REPUBLIC

Prof. Dr. Khanh Chau Le
Lehrstuhl für Allgemeine Mechanik
Ruhr-Universität Bochum
Fakultät für Bauingenieurwesen
Universitätsstr. 150
44801 Bochum
GERMANY

Prof. Dr. Tony Lelievre
CERMICS - ENPC
Cite Descartes, Champs-sur-Marne
6 et 8 avenue Blaise Pascal
77455 Marne-la-Vallee Cedex 2
FRANCE

Prof. Dr. Stephan Luckhaus
Mathematisches Institut
Universität Leipzig
Postfach 10 09 20
04009 Leipzig
GERMANY

Prof. Dr. Alexander Mielke
Weierstraß-Institut für
Angewandte Analysis und Stochastik
Mohrenstr. 39
10117 Berlin
GERMANY

Prof. Dr. Ingo Müller
Institut für Verfahrenstechnik
FG Thermodynamik
Technische Universität Berlin
Fasanenstr. 90
10623 Berlin
GERMANY

Prof. Dr. Michael Ortiz
Division of Engineering and
Applied Sciences, MS 104-44
California Institute of Technology
Pasadena, CA 91125
UNITED STATES

Prof. Dr. Felix Otto
Max-Planck-Institut für Mathematik
in den Naturwissenschaften
Inselstr. 22 - 26
04103 Leipzig
GERMANY

Prof. Dr. Mark A. Peletier
Department of Mathematics
Eindhoven University of Technology
P.O.Box 513
5600 MB Eindhoven
NETHERLANDS

Dr. Francisco-Jose Perez-Reche
Inst. for Complex Systems & Math.
Biology
School of Natural and Computing
Sciences
University of Aberdeen
Dunbar Street
Aberdeen, AB24 3UE
UNITED KINGDOM

Prof. Dr. Luigi Preziosi
Dipartimento di Scienze Matematiche
Politecnico di Torino
Corso Duca degli Abruzzi, 24
10129 Torino
ITALY

Dr. Giuseppe Puglisi
Dipartimento di Ingegneria ed
Ambientale
Politecnico di Bari
Via Orabona, 4
70125 Bari
ITALY

Pierre Recho
Institut Curie
Physico-Chimie Curie
11, rue Pierre et Marie Curie
75005 Paris
FRANCE

Prof. Dr. Phoebus Rosakis
Department of Applied Mathematics
University of Crete
70013 Heraklion, Crete
GREECE

Dr. Eris Runa
Max-Planck-Institut für Mathematik
in den Naturwissenschaften
Inselstr. 22 - 26
04103 Leipzig
GERMANY

Dr. Giuseppe Saccomandi
Dipartimento di Ingegneria
Universita degli Studi di Perugia
Via G. Duranti, 1
06125 Perugia
ITALY

Dr. Oguz Umut Salman
Dip. di Matematica e Applicazioni
Universita di Milano-Bicocca
Edificio U5
via Roberto Cozzi 53
20125 Milano
ITALY

Dr. Andre Schlichting
Institut für Angewandte Mathematik
Universität Bonn
Postfach 2220
53115 Bonn
GERMANY

Prof. Dr. Bernd Schmidt
Institut für Mathematik
Universität Augsburg
86135 Augsburg
GERMANY

Prof. Dr. Peter Smereka
Department of Mathematics
The University of Michigan
530 Church St.
Ann Arbor, MI 48109-1109
UNITED STATES

Prof. Dr. Valery P. Smyshlyaev
Department of Mathematics
University College London
Gower Street
London WC1E 6BT
UNITED KINGDOM

Prof. Dr. Florian Theil
Mathematics Institute
University of Warwick
Zeeman Building
Coventry CV4 7AL
UNITED KINGDOM

Prof. Dr. Lev Truskinovsky
Lab. de Mecanique des Solides
UMR-CNRS 7649
École Polytechnique
91128 Palaiseau Cedex
FRANCE

Prof. Dr. Anna Vainchtein
Department of Mathematics
University of Pittsburgh
301 Thackery Hall
Pittsburgh, PA 15260
UNITED STATES

Dr. Patrick J.P. van Meurs
Dept. of Mathematics & Computer Science
Eindhoven University of Technology
5600 MB Eindhoven
NETHERLANDS

Dr. Guido Vitale
Lab. Interdisciplinaire de Physique
Université Joseph Fourier
BP 53
38041 Grenoble Cedex 9
FRANCE

Dr. Jens Wohlgemuth
Max-Planck-Institut für Mathematik in den Naturwissenschaften
Inselstr. 22 - 26
04103 Leipzig
GERMANY

Prof. Dr. Arash Yavari
School of Civil and Environment Eng.
Georgia Institute of Technology
790 Atlantic Drive
Atlanta GA 30332-0355
UNITED STATES

Dr. Giovanni Zanzotto
Dip. di Metodi e Modelli Matematici
Universita di Padova
Via Trieste, 63
35121 Padova
ITALY

Dr. Giuseppe Zurlo
Lab. de Mecanique des Solides
UMR-CNRS 7649
École Polytechnique
91128 Palaiseau Cedex
FRANCE